TIME VARIATIONS OF MAGNETOSPHERIC INTENSITIES OF OUTER ZONE PROTONS, ALPHA PARTICLES AND IONS (Z > 2)*

by

Bruce A. Randall

Department of Physics and Astronomy

THE UNIVERSITY OF IOWA

Iowa City, Iowa

U. of Iowa 73-3

TIME VARIATIONS OF MAGNETOSPHERIC INTENSITIES OF OUTER ZONE PROTONS, ALPHA PARTICLES AND IONS ($Z > 2$)*

by

Bruce A. Randall

Department of Physics and Astronomy
The University of Iowa
Iowa City, Iowa 52242

January 1973

*This research was supported in part by the National Aeronautics and Space Administration under contract NAS1-8141 and by the U. S. Office of Naval Research contract N00014-68-A-0196-0003.

ABSTRACT

A comprehensive study of the temporal behavior of trapped protons, alpha particles and ions ($Z > 2$) in the outer zone of the earth's magnetosphere has been made. These observations were made by the Injun V satellite during the first 21 months of operation, August 1968 to May 1970. Rapid increases in the observed number of particles followed by slower exponential decay characterize the data. Comparisons are made with the temporal behavior of interplanetary particles of the same energy observed by Explorer 35. Increases in the trapped fluxes generally correspond to enhanced interplanetary activity. The energy spectra of protons and alpha particles at $L = 3$ have similar shapes when compared on an energy per charge basis while the respective polar cap spectra have similar shape on an energy per nucleon basis. Apparent inward trans-L motion of energetic protons is observed. The temporal association of interplanetary particles, the apparent trans-L motion and the charge dependence of the energy spectra lead one to believe that the source of increases of trapped particles is energetic solar particles penetrating to the polar cap. These particles are diffused inward by a process involving fluctuating electric fields. The loss of trapped low altitude protons, alpha particles and ions ($Z > 2$) is controlled by coulombic energy loss in the atmosphere.

I. INTRODUCTION

Since the discovery of the trapped radiation belts 14 years ago, many subsequent observations (Heckman and Armstrong, 1962; Davis and Williamson, 1963; Mihalov and White, 1966; Fillius, 1966; Frank and Owens, 1970; Pizzella and Randall, 1971) have determined the intensities, energy spectrum and distribution of the outer zone trapped protons. Alpha particle observations are much less extensive than proton observations, covering an energy range of about 1 to 10 MeV, and only a crude knowledge has been gained of the differential energy spectrum (Krimigis and Van Allen, 1967; Paulikas and Blake, 1968; Fritz and Krimigis, 1969; Van Allen and Randall, 1971); but these results do indicate that alpha particles of these energies are distributed in L in about the same manner as protons with energies of 0.3 to 10 MeV. The ratio of intensities of alpha particles to protons with 300 keV kinetic energy per nucleon has been found to be on the order of 10^{-4} (Krimigis, 1970). The measurements of heavier ions ($Z > 2$) are very preliminary (Krimigis et al., 1970; Van Allen et al., 1970) but they seem to have a similar distribution in L as protons and alpha particles with kinetic energies of 300 keV per nucleon.

The nature of the source and loss mechanisms of particles in the magnetosphere and the low ratios of intensity of alpha particles

to protons and of ions ($Z > 2$) to alpha particles compared to the solar wind values remains comparatively obscure. The extensive data from Injun V and Explorer 35 provide a unique opportunity to observe the dynamics of the magnetosphere and its interaction with interplanetary particles and possibly infer from these observations the source and loss mechanisms and the reasons for the low ratio of intensities.

The Injun V solid state experiment gives good spectral information on protons in the outer zone with 10 channels covering the energy range 0.3 to 74 MeV (Pizzella and Randall, 1971). The alpha particle detector has three nested energy passbands from which limited spectral information can be obtained and the relationship between the proton and alpha particle energy spectra can be examined. The ion ($Z > 2$) measurements come from a single energy passband, but these are useful in determining intensity ratios with the more abundant species of particles once a spectral form is determined. The ability to determine the energy spectra of particles, coupled with the long life time of $\sim$ 21 months and large quantity of data gives a good sampling of particle intensities as a function of time in the outer zone, and in the auroral and polar cap regions.

Explorer 35 is in a lunar orbit and carries a solid state detector experiment which has two nested proton passbands, .32 to 6.3 MeV, an alpha particle passband and a channel for detecting ions ($Z > 2$). The data from these energy passbands give the activity in

interplanetary space and can be compared with the Injun V data over the polar caps.

The purpose of this paper is to determine the energy spectra of protons, alpha particles and ions ($Z > 2$) and to do a time study of the data from the two experiments and to attempt to determine the mechanisms for the origin and loss of protons, alpha particles and ions ($Z > 2$) in the magnetosphere.

II. EXPERIMENT

Injun V is a low altitude, polar orbiting satellite that was launched on 8 August 1968 with an initial perigee altitude of 644 km and an apogee altitude of 2525 km. The orbit has an inclination of 81 degrees and the initial period was 118 minutes. The satellite achieved continuous alignment (± 15°) with the earth's magnetic field by 16 December 1968, after tumbling for several months. Prior to this time, the data were selected if the on-board magnetometer indicated that the detector was aimed 90° ± 10° to the field lines. After this time the detectors were always aimed approximately orthogonal to the local field lines. Thus all of the observations of the geomagnetically trapped particles are for particles mirroring at or near the altitude of the satellite.

The experiment consists of two separate detector systems, the proton-electron telescope and the alpha particle detector. The proton-electron telescope has for its first element a 24.1 micron thick, totally depleted surface barrier silicon detector with an area of 10.1 mm^2. The collimator has a half angle of 14.5°. Behind this detector are two more detectors with thickness of 862 and 905 microns as shown in Figure 1. These detectors are used for counting electrons, high energy protons and as a coincidence system with the first detector. The system works in two basic modes. One mode does not use the coincidence system and has four nested

proton energy passbands from the first detector and four nested electron energy passbands from the second and third detectors plus two nested higher energy proton passbands. The other mode uses the coincidence system, which places a common upper level on the four low energy passbands and eliminates protons penetrating the thin detector from being counted as electrons. The two higher energy passbands remain unaffected by the coincidence system. (See Figure 2.)

The alpha particle experiment consists of an 8.5 micron thick, totally depleted surface barrier silicon wafer, with an area of 3.1 mm^2 and a collimator opening angle of 26.5° as shown in Figure 3. The detection scheme is similar to that of the previous system. Three of the discrimination levels are set for alpha particles and one more is set for ions with $Z > 2$. The alpha particle levels are set such that the lowest level is 300 keV higher than the maximum energy loss for protons in the detector. The ion level is set one MeV higher than the maximum energy loss for alpha particles in the same detector. (See Figure 4.) The pulses from this detector are delay line clipped to 100 nanoseconds and the pulses can be resolved if they occur more than 54 nanoseconds apart. Both detector systems have brass apertures which give shielding of approximately 100 MeV for protons not coming through the opening angle. For more detailed information on this detector system, see Randall (1969).

Explorer 35 is a lunar orbiting satellite which is oriented with its spin axis orthogonal to within 7° to the ecliptic plane. The data are sectored into four equal sectors with Sector III looking toward the sun. This satellite carried a similar experiment package as described above. The detector is a 20 micron thick, totally depleted silicon surface barrier junction, with an area of 10 mm^2. The collimator is a cone with a half angle of 30° and brass side shielding sufficient to stop 50 MeV protons. The energy levels are set such that there are two nested proton energy passbands, an alpha particle energy level and an ion ($Z > 2$) energy level (Figure 5). The electronics are basically the same as previously described, with the exception that this experiment can resolve two events only if they are separated in time by more than 120 nanoseconds (Van Allen and Ness, 1969). The pertinent energy passbands and geometric factors for all of the experiments are summarized below:

Injun V Proton-Electron Telescope

P_1	.304	$\leq E_p \leq$	9.2	MeV
P_2	.448	$\leq E_p \leq$	4.21	MeV
P_3	.63	$\leq E_p \leq$	2.64	MeV
P_4	.80	$\leq E_p \leq$	1.94	MeV
P_5	.306	$\leq E_p \leq$	1.43	MeV
P_6	.45	$\leq E_p \leq$	1.43	MeV
P_7	.63	$\leq E_p \leq$	1.43	MeV
P_8	.80	$\leq E_p \leq$	1.43	MeV
P_9	3.44	$\leq E_p \leq$	74	MeV
P_{10}	8.42	$\leq E_p \leq$	24.9	MeV

Geometric Factor = 0.020 cm^2 sr

Injun V Alpha Particle Detector

A_1	1.18	$\leq E_\alpha \leq$	8.4	MeV
A_2	1.60	$\leq E_\alpha \leq$	5.0	MeV
A_3	2.0	$\leq E_\alpha \leq$	3.5	MeV
A_4	4.6	$\leq E_C \leq$	85	MeV
	4.7	$\leq E_N \leq$	140	MeV
	5.0	$\leq E_O \leq$	24.9	MeV

Geometric Factor = 0.0051 cm^2 sr

Explorer 35

P_1	0.32	$\leq E_p \leq$	6.3	MeV
P_2	0.48	$\leq E_p \leq$	3.0	MeV
P_3	7.0	$\leq E_C \leq$	114	MeV
	7.1	$\leq E_N \leq$	196	MeV
	7.5	$\leq E_O \leq$	304	MeV
P_4	2.0	$\leq E_\alpha \leq$	10.2	MeV

Geometric Factor = 0.079 cm^2 sr

Since the basic characteristics of the detector system have been described, it is of interest to consider possible problems that might be encountered in an analysis of the data. The following processes which could pose potential problems have been discussed at some length by Krimigis and Van Allen (1967) for a similar detector system: (a) pulse pileup, (b) transverse penetration, (c) elastic scattering, and (d) inelastic nuclear interaction.

With regard to the Injun V experiment these processes have been evaluated as follows: Process (a), the proton experiment, was tested prior to flight using a 1 curie Sr^{90} β^- source and it was determined that pileup was due to a four-fold coincidence of electrons with energies between 50 and 100 keV. The integral flux of electrons with these energies found in the outer zone can be found by extrapolating the electron spectra of Randall (1969). These results show that the flux is less than 5×10^6 electrons cm^2 sec sr and would contribute less than one count per second to the lowest energy proton channel. The alpha particle detector is not sensitive to electrons but the lowest alpha particle energy level is set at 900 keV and a two-fold coincidence of protons with energies between 0.45 and 1.2 MeV could give spurious counts. The effect due to this is given by

$$R_\alpha = \tau R_p^2 \exp(-R_p \tau)$$

where $\tau = 1.08 \times 10^{-7}$ seconds and R_p is the counting rate of protons with energies between .45 and 1.2 MeV. The second proton energy level counts protons with energies between 0.45 and 1.43 MeV and the maximum counting rate was observed to be about 5000 counts per second. Accounting for the differences in geometric factors, the contribution to the lowest alpha particle energy level is 0.17 counts per second. When this maximum proton rate was observed in flight, the lowest alpha particle energy level was counting approximately 10 counts per second so the contribution from this effect is negligible. The ion ($Z > 2$) energy level is set about six times higher than the maximum energy loss for protons in the thin detector, so the only possibility to have pileup is to have two or more alpha particles be coincident. Assuming maximum rate of 20 counts per second due to alpha particles leaving 1.75 MeV or greater in the thin detector, the contribution to the ion ($Z > 2$) energy level would be 4.3×10^{-5} counts per second. The ion to alpha particle intensity ratio would then be less than 2.2×10^{-6}, whereas the observed ratios are about 1000 times larger as can be seen in Figure 17. Thus process (a) is negligible for the Injun V experiment.

For process (b), the transverse penetration of the collimator and detector by high energy particles, the problem does not exist in the outer zone since the flux of protons with energies greater than 95 MeV mirroring at Injun V altitudes is less than 10^{-5} protons/ cm^2 seconds sr (Pizzella and Randall, 1971).

Process (c), elastic scattering, was tested for the alpha particle detector during the initial calibration. A 10 micron thick detector, in the same configuration as used in flight, was bombarded with 0.95 to 1.2 MeV protons which is greater than the 900 keV threshold at rates of less than 50 protons per second incident on the detector. The efficiency for counting these protons was less than 0.03% (Randall, 1969). The actual efficiency for the flight detector should be smaller since the detector used is thinner. The contamination due to elastic scattering for the ion ($Z > 2$) energy level is much smaller since the energy loss necessary to trigger this level is 3.5 MeV and according to Janni (1966), the percent of multiple scattering for protons of 3.5 MeV is reduced by a factor of 1.39 from that for 1 MeV protons. Alpha particles, since they are more ionizing, should produce the biggest effect but assuming an efficiency of 0.1%, the contribution from alpha particles with energies greater than 3.5 MeV would be 2.2×10^{-4} counts per second, if the first alpha particle energy level was counting 10 counts per second. This would give an ion ($Z > 2$) to alpha particle intensity ratio of 2.2×10^{-5}, which is much smaller than the observed results in Figure 17. The ions ($Z > 2$) also have a very different L dependence from that of the high energy protons (Van Allen et al., 1970). Mutliple scattering of low energy electrons could affect the low energy proton detector but it has been determined experimentally that contributions from this effect would require a two-fold coincidence and are quite negligible in the outer zone.

For process (d), inelastic nuclear interaction, the probability of an inelastic nuclear interaction taking place in the detector or collimator is less than 0.0002 for protons less than 5 MeV (Janni, 1966).

These same problems were potentially present for the Explorer 35 experiment and have been discussed by Armstrong and Krimigis (1971). They also conclude that the detector system on Explorer 35 is counting what it was designed to count.

III. DATA ANALYSIS

The Injun V solid state detector data were first stripped from the master data file and a new file was created. These tapes had all of the orbital parameters and count rates of each detector energy level in counts per frame. From this file a master SSD file was created by doing a 15 second average on all of the data. This resulted in approximately 4.27×10^5 records of data each containing all of the orbital parameters and 24 different measurements of energetic particles. This averaging was desirable since the experiment operated by sequencing through the various possible modes and 15 seconds represented the shortest division in which data were available from all modes. Before magnetic orientation was obtained, the data were selected if the orientation of the detector axis as indicated by the magnetometer was within 10° from being orthogonal to the local magnetic field. The quantity of data improved markedly after orientation since it was not necessary to discard data due to the orientation of the satellite.

The data reduction for the time study part of this paper then involved sorting the outer zone data into small sections in L space. The data within each interval were then averaged. Six different L bins were used. Thus it is possible to obtain 24 different samples per orbit. The following intervals were used:

$$L = 2.5 \pm 0.25$$
$$3.0 \pm 0.25$$
$$3.5 \pm 0.25$$
$$4.0 \pm 0.25$$
$$5.125 \pm 0.875$$
$$6.6 \pm 0.60$$

During eight geomagnetically quiet periods, these data were then analyzed using a two variable least squares fit in magnetic field B and in time T. The equation for the fit is

$$\log (\text{count rate}) = A_1 + A_2 B + A_3 B^2 + A_4 T.$$

This fit assumes that the fluxes of particles vary as an exponential in time and is based on the results of a preliminary time study which used the data from a given L shell and a very small range of magnetic field strength. The second order polynomial in B has been used before (Pizzella and Randall, 1971) and quite adequately fits the data. This fit accomplished two things: First, it made it possible to convert all of the observed data to a common value of magnetic field such that a study of the time variations could be made. It also yielded values of the decay times of the various species of particles. These data were adjusted to a value of $B = 0.20$ if $0.15 \leq B \leq 0.33$ and averaged on a daily basis. The final

plots of the data were produced using a running three-point average for smoothing out statistical fluctuations. The plots for L = 6.6 were not smoothed because the fluctuations are believed to be real and the data gaps were more numerous. The heavy ion data had to be handled in a different manner since the fluxes were so low. These data were selected on the criteria that L = 3.25 ± 1.0 and B = 0.20 ± 0.03 and then averaged by hand to eliminate any possibility of spurious counts contaminating the results. Ten day averages were picked to obtain the best statistics and yet say something about the time behavior of these particles. The comparison alpha-particle data were analyzed in the same manner.

IV. OBSERVATIONS

A. Time History

Data are available from the solid state detector experiment from 29 August 1968 to 29 May 1970. During this time period the peak of the sunspot cycle occurred thus giving rise to a wide variety of geophysical phenomena, from quiescent periods to massive solar and geophysical storms. A time history study of several species of particles should give some insight into the working of the magnetosphere.

Figure 6 gives a time survey of protons 0.3 to 9.1 MeV at L = 3 as seen by Injun V and interplanetary fluxes of protons 0.32 to 6.3 MeV as seen by lunar orbiting Explorer 35. It is important to note that the trapped fluxes at L = 3 vary during this time period by more than a factor of 10 and that all increases occur not in periods of a month but in only a few days. These enhancements always seem to occur in association with an increase in the interplanetary particles of the same energy, but an increase in interplanetary flux does not always have an associated increase in the trapped fluxes.

From Figures 7 and 8 it is clear that the interplanetary fluxes of alpha particles and ions ($Z > 2$) increase at the same

time as do the proton fluxes but the intensity ratios of protons to alpha particles and alpha particles to ions vary considerably from event to event and even during a single event (Van Allen et al., 1971; Armstrong and Krimigis, 1971).

The worldwide geomagnetic activity as characterized by A_p seems to be correlated with increases in the interplanetary fluxes and high values of A_p do seem to be related to abrupt changes in the trapped particles as can be seen from Figures 6 and 7.

The alpha particle flux at L = 6.6 as seen in Figure 9 shows no durably trapped intensity but only brief transient peaks caused by interplanetary particles. This same phenomenon is observed at synchronous orbits as has been reported by Lanzerotti (1970), Sevens et al. (1970) and Paulikas and Blake (1969).

Figures 10 through 13 show the alpha particles on decreasing L shells. A great amount of variation of intensity as a function of time can be seen in the data. The intensity increases occur within a few days, while decreases take place slowly over several weeks. This slow decay characterizes stably trapped particles, whereas the quasi-trapped or non-trapped particles at L = 6.6 have an altogether different time behavior.

Figure 14 exhibits the same general character for the ions but it has the additional feature that there were no ions observed with Injun V from the beginning of the observations until day 303, 1968. The early period comprises only 4962 seconds of data for which one count would represent a rate of 2.2×10^{-4} counts per second.

After this time there was an influx of energetic ions ($Z > 2$) from either the earth's atmosphere or the solar wind, that increased the observed flux by a factor of the order of 100.

If the source of the ions was the atmosphere then the particles would have had to have been accelerated from essentially thermal energies to 5 MeV in the period of just a few days since days 295, 296 and 297 were three of the five quietest days during the month. This time period seems to be too short for any of the mechanisms thus far proposed to accelerate particles to such energies (Pizzella, 1970).

Since the atmosphere does not seem to be the source of particles, it is best to look for a solar origin since the observed increase in the outer radiation zone seems to occur at the same time as increases in the interplanetary fluxes. Figure 15 is a typical example of a polar cap pass. Other examples can be found in the literature such as Van Allen et al.,(1971), Krimigis and Van Allen (1967), Reid and Sauer (1967), and Evans and Stone (1969). This exemplary pass was on day 272, 1969 and the more or less quiescent pass was on day 262 and covered the same B, L space so it can give a baseline with which to compare the trapping boundaries. During this disturbed time the polar plateau was immersed in particles and the counting rates of the protons and alpha particles observed by Injun V agree very well with the observed interplanetary fluxes of protons and alpha particles seen by Explorer 35.

The protons during this event were observed to have an approximately constant intensity from the polar cap down to an invariant latitude of 60°, where it becomes impossible to distinguish them from the outer zone protons on any simple basis. The alpha particle intensities drop off at about 63 or 64° invariant latitude such that it is easy to distinguish between the trapped and quasi-trapped alpha particles. The alpha particle observations definitely show that the quasi-trapped alpha particles are not of magnetospheric origin since they are of the same intensity as seen by Explorer 35 and are higher than the trapped fluxes. The polar cap protons are certainly of interplanetary origin. Thus observations show that during solar particle events, particles with energies as low as 0.3 MeV per nucleon can directly penetrate to as low as 63° invariant latitude which is the quasi-trapping region and that definite increases sometimes occur within at most a few days. The shortness of this time scale is exemplified by the observations on 1 November 1968 reported by Van Allen and Randall (1971), where alpha particle intensities increased by a factor of 12 within the observational resolution time of 13 hours at L = 3.25 ± 0.25 and B = 0.20 ± 0.025.

The ratios of the particle intensities in the outer zone are shown in Figures 16 and 17. The ratio of intensities of alpha particles to that of protons shows a remarkable variability. During these observations it changed by a factor of 20. These are very sharp increases in the ratio which correspond to the abrupt increases

in the particle intensities and to the solar particle events. The decay rate of the ratio appears to be composed of two components, a short decay rate superimposed on a longer rate. Both decay rates can be represented by simple exponentials. The long decay time is about 100 days while the shorter is approximately 30 days. The different rates of decay indicate that there are at least two different loss processes taking place. The ion ($Z > 2$) to alpha particle intensity ratio has much statistical uncertainty but is apparently less variable than the alpha particle to proton ratio. The alpha particle to proton intensity ratio in interplanetary space during solar particle events has been shown to be highly variable whereas the ion to alpha particle ratio is considerably less so according to Van Allen et al. (1971) and Armstrong and Krimigis (1971). From their figures the alpha particle to proton intensity ratio is about 2×10^{-2} for 0.5 MeV per nucleon particles and the ion to alpha particle intensity ratio is about 5×10^{-2} for 0.5 MeV per nucleon particles. The observed intensity ratios in the magnetosphere at $L = 3$, $B = 0.2$ for 0.3 MeV per nucleon particles are about 4×10^{-4} for alpha particles to protons and about 2×10^{-3} for ions to alpha particles.

The time history of the alpha particle intensity is worth considering again since there are many details that have not been discussed above. At $L = 4$ the alpha particle intensity shows variability but decays much more quickly than at the lower L shells, to

approximately a constant level of 0.1 counts per second. The sudden depressions are of some interest since they might represent slight momentary losses or redistributions of particles during one phase of a geomagnetic storm. At lower L shells (3.5 and 3) the increases become much larger than at L = 4 and the subsequent decay times are longer.

One of the more interesting events and one that has not been covered in the literature occurred around day 134, 1969. The interplanetary fluxes of protons and alpha particles were fairly high, 350 counts per second for proton with energies 0.32 to 6.3 MeV and 5.8 counts per second for alpha particles with energies 2.0 to 10.2 MeV for a daily average. The magnetic index A_p was 131 and comparable intensities of particles were observed over the polar caps with Injun V. The proton intensities were very much like that shown in Figure 15 in that they blended smoothly into the outer zone proton belt. The intensities of the alpha particles increased at L = 6.6 and L = 4 as seen in Figures 9 and 10. The intensities decreased at L = 3.5, 3 and 2.5 and the alpha particle to proton ratio at L = 3 also decreased. The interest in this particular event is that the mechanism which caused increases in trapped particles during other events also produced losses from the usual trapping zone. The intensities at L = 6.6 (Figure 9) remained high for several days after which the intensities at L = 3.5 and 3 increased slightly and at L = 2.5 the intensities remain about the same.

B. Spectra

To realistically compare alpha particle intensities to those of protons and also to the heavier charged ions, it is desirable to know the energy spectra of the various species. Since the Injun V experiment has only three nested alpha particle channels and only one heavy ion channel it is not possible to obtain directly any precise spectral information. It is possible to integrate simple spectral forms over the energy range and to use the ratios of the actual data to determine the spectral form which best fits the data. However, in most cases these simple spectra (e.g., a power law or an exponential) are useful only over a short interval.

Another possible method is to construct an integral spectrum from the proton data, such as Figures 18, 19 and 20, and them assume that the alpha spectrum is similar and to graphically determine the contribution to each alpha channel from such a spectrum. The three comparisons that have been made are on the basis of the same kinetic energy per nucleon, the kinetic energy per charge or finally, the same kinetic energy.

At $L = 3.0 \pm 0.25$ and $B = 0.20 \pm 0.015$, a comparison of the ratios of the experimental data with the ratios obtained graphically from 11 integral proton spectra made approximately 30 days apart are summarized below.

	Ratio A_2/A_1	Ratio A_3/A_1
Experimental Data	0.400	0.122
Energy per Nucleon	0.557	0.282
Energy per Charge	0.389	0.149

A comparison of the calculated ratios made by numerically integrating the experimental proton energy spectrum over the alpha particle passbands, indicates that the proton and alpha particle spectra are not similar in shape on an energy per nucleon basis. This is important since most published reports on the alpha particle to proton ratio have been made assuming that this is the correct mode of comparison.

A comparison of spectra on an energy per charge basis gives ratios which agree within the statistical errors of the data. The comparison on the same kinetic energy basis yields ratios about the same as the comparison with the same kinetic energy per charge. This is due to the fact that the energy spectra had to be extrapolated to higher energies to take into account the upper thresholds. Errors involved in doing this are great but do not exclude the comparison on the same kinetic energy basis as a possibility. In an attempt to distinguish between these two possibilities, the integral proton spectra were graphically fit to the integral of the following differential spectrum:

$$\frac{dJ}{dE} = \sqrt{E/E_*} \exp\left(-\sqrt{E/E_*}\right)$$

This spectral form due to Pizzella was chosen since it has been shown to fit the outer zone proton spectra over a wide range of energies (Pizzella et al., 1970; Pizzella and Frank, 1971). From this graphical comparison a value of E_* was determined for each proton spectrum and the subsequent integrations over the alpha particle energy passbands gave the following average ratios: $A_2/A_1 = 0.421$ and $A_3/A_1 = 0.183$ for the energy per charge comparison and $A_2/A_1 = 0.271$ and $A_3/A_1 = 0.089$ for the kinetic energy comparison. The A_2/A_1 ratio for the energy per charge comparison agrees within the statistical errors of the experimental data ratio. The A_3/A_1 ratio for the energy per charge comparison is higher than the experimental ratio but the consistent agreement of the A_2/A_1 ratio for the energy per charge comparison with the experimental ratio tends to favor this basis of comparison.

It is of further interest to determine the form of the polar cap differential energy spectra during solar particle events. Ten different events were analyzed and the integral proton spectra were constructed. All of the spectra had the same basic shape, which was not a simple power law or an exponential, but was in general a slowly falling spectrum, indicating many high energy protons. An attempt was then made to see how the alpha particle spectra were related to

the proton spectra. Due to the shape of the spectra all of the ratios found by integration of the proton spectra were the same within the statistics of the experimental data. Thus it was impossible to determine how the polar cap alpha particle spectra compared with the proton spectra.

A typical comparison of experimental data with the ratios obtained graphically from the integral proton spectrum is shown below.

	Ratio A_2/A_1	Ratio A_3/A_1
Experimental Data	0.580 ± 0.054	0.245 ± 0.030
Energy per Nucleon	0.603	0.301
Energy per Charge	0.581	0.283
Energy	0.655	0.329

The proton fluxes in interplanetary space measured by Explorer 35 were then compared with the polar cap proton spectra. The ratio of P_2/P_1 for Explorer 35 during this time was 0.649. The ratio of the integrals of the polar cap spectrum over the Explorer 35 passband was 0.637. This then means that protons from interplanetary space have direct access to the polar caps and that the energy spectra are not measurably changed in the process over the enery range 0.32 to 6.3 MeV. The alpha particle to proton intensity ratio was then calculated using both energy per nucleon and energy per charge for the alpha particle energy ranges on Explorer 35 and Injun V. The most consistent agreement among the four energy passbands for a

constant ratio was with the energy per nucleon comparison. If the ratio varies with energy then the spectra are not similar in shape. The energy per nucleon comparison seems to be in agreement with the higher energy observation of Lezniak and Weber (1971).

The two heavy ion channels also give similar values for the ion to proton ratio for an assumed similarity of spectra on an energy per nucleon comparison.

The similarity of the proton and alpha particle energy spectra on an energy per charge basis at L = 3, and the apparent fact that the polar cap spectra are related in a different manner and have a higher average energy, indicated that some physical process depending on the particle's charge must have taken place. Whalen et al. (1971) have shown that the low energy auroral ions have similar energy spectra when compared on an energy per charge basis, thus adding more evidence to support the outer zone results.

C. Diffusion

If the source of the outer zone particles is the solar wind during disturbed times, then it might be possible to observe trans-L motion of these particles. An attempt was made to see if this was the case. Irregularities such as statistically significant bumps in the radial distribution of 0.3 to 1.43 MeV proton were looked for and when found, a search for similar occurrence on the next satellite pass through the same local time and approximate magnetic field strength was made. If such an event occurred, the difference in the L shells divided by the difference in time between measurements was taken as the diffusion velocity of the particles, $\Delta L/\Delta t$. Figure 21 shows the fruits of this labor, that is, the values of $\Delta L/\Delta t$ vs L.

As an example, the first point was found on day 135, 1969 at 17:12.1, at which time the counting rate at L = 10.61 was 4 σ higher than the next 2.5 minutes of data. Two revolutions later at 21:02.6 a peak in the counting rate, again 4 σ higher than the background, occurred. The L value was 7.63 so the value of $\Delta L/\Delta t$ is $(10.61 - 7.63)/3.84 = 0.776$ hour^{-1}. The other six points were found in a similar manner.

The straight line fit shows that $\Delta L/\Delta t$ decreases sharply as L becomes smaller. These data represent a trans-L diffusion since Injun V is polar orbiting and each set of measurements was taken at approximately the same altitude. It seems to represent an

equatorward convection of sets of disturbances. The extrapolation to lower L shells is intriguing, but is virtually impossible to observe experimentally due to the slowness of the motion of the orbit in B, L, and MLT space.

V. INTERPRETATION OF THE OBSERVATIONS

A. The Source

From the data presented, the time histories of the outer zone protons, alpha particles and ions ($Z > 2$) can be characterized as follows: The intensities increase sharply on the time scale of a day or two; decreases in intensity appear to be exponential to a first approximation and have a time scale on the order of weeks. The initial increases represent an increase in the number of particles observed in the outer zone and the excess number of particles should be explained.

Possible explanations that have been suggested are a redistribution of the equatorial pitch angles, diffusion outward from the atmosphere, diffusion inward from the solar wind, and direct capture. The data from Injun V cannot be used to determine if the increases are due to a redistribution of equatorial pitch angles. For such a determination it would be necessary to have simultaneous observations at the equator and at low altitudes and such data do not seem to be available. The diffusion outward from the atmosphere (Pizzella, 1970) does not take place rapidly enough to account for the observations. A number of radial diffusion theories using the solar wind as a source have been proposed in the past by Davis and Chang (1962), Tverskoy (1964), and Nakada and Mead (1965),

and these have been extended by others in recent years. But there is some doubt that these mechanisms operate quickly enough to produce results which would be consistent with the present set of data. These mechanisms may account for a gradual diffusion of particles into the trapping regions and could be the source for the more stable inner zone.

Other radial diffusion theories using electrostatic fluctuations have been suggested (Cornwall, 1968, 1972; Fälthammar, 1965, 1968; Birmingham, 1969; Cole, 1971) and such a process would be charge dependent but these calculations also indicate that the process would be too slow to account for the present observations. The similarity of the outer zone particle spectra when compared on an energy per charge basis and the different dependence found over the polar caps indicate that the transport process must depend on electric fields, since this is the probable means by which such a transformation would be dependent on the charge of the particle. The problem involved with a direct transport is that the polar cap spectra have a much higher average energy than the spectra at L = 3. Both spectra can be fairly well approximated by Pizzella's spectrum (Figures 18, 19 and 20) where E_* is on the order of 90 keV over the polar cap and about 13 keV at L = 3. The data published by Pizzella and Frank (1971) showed that the value of E_* decreases as a function of increasing L. Thus direct capture of particles in the simplest sense seems unlikely since the energy spectra are quite different, thus indicating that the particles must undergo some transport process.

During events such as in Figure 15, the value of E_* is fairly constant from an invariant latitude of 65° on out to 90°. For this event the value of E_* was about 40 keV over the whole range of latitudes for protons. The statistics over such short time periods prevent one from determining very much quantitatively with the protons and a larger time interval would necessitate a larger spatial average, and as can be seen from Figure 15, the rates do vary spatially.

Thus it would appear that the source for the increases observed in the outer zone could be from these particles which have direct access down to about 65° invariant latitude. The mechanism that then moves these particles into the stable trapping region from this apparent boundary must depend on the charge of the particle because of the similarity of the differential energy spectra of the various species when compared on an energy per charge basis. If the low altitude auroral region were the source for one of the diffusion mechanisms, the particles would not have to be energized as much as in equatorial diffusion since the magnetic field is much higher and the first adiabatic invariant could still be preserved.

Since the transport mechanism appears to be charge dependent, it is of interest to look at one of the models in greater detail. Cornwall's (1972) model for such a diffusive process gives diffusion

rates too low by several orders of magnitude to account for the fast increases observed in the Injun V data. But this model used input data from relatively quiet times rather than for disturbed times during which major increases were observed. Cornwall's assumed source is the solar wind plasma. If the input parameters were changed such that they reflected very disturbed times, it might help, but the real problem lies in the L dependence of the diffusion coefficient. The observed dependence on $\Delta L/\Delta t$ is $\alpha L^{3.2}$ (Figure 21). The diffusion coefficient should then be proportional to $L^{4.2}$. Cornwall's much steeper dependence on L would result in a much slower diffusion than is observed. But the observed data were taken by looking at the apparent motion of disturbances in the distribution of 0.3 to 1.43 MeV protons, whereas the model has energies of the particles continually increasing by conservation of the first adiabatic invariant. If Cornwall's diffusion coefficient is evaluated at various values of L for a constant energy, one finds that the coefficient is proportional to L^4. Following the analysis of Fälthammer (1968), the diffusion coefficient

$$D = \frac{1}{2} \frac{\langle (\Delta L)^2 \rangle}{\Delta t}$$

and for $D = K L^4$ then $\frac{\Delta L}{\Delta t} = 2K L^3$. The value of 2K from this analysis is 1.4×10^{-5} for a 300 keV proton and the value decreases rapidly with increasing energy.

Thus it appears that Cornwall's model is definitely a step in the right direction, in that the diffusion coefficient depends on L in the same way as the observation. If the coefficients are evaluated during storm time and the source of particles is taken to be energetic solar particles that have penetrated to the polar cap region, the results might be in agreement.

B. Losses

The data presented as the long time histories of protons, alpha particles and ions ($Z > 2$) show that the decay in intensity of these particles after an impulsive increase is exponential to first order. For the decay periods in which the magnetic activity is very low, one finds that the decay time for protons (0.3 to 9.2 MeV) at $L = 3$ and $B = 0.2$ is 30.3 ± 1.7 days. The alpha particles (1.18 to 8.4 MeV) under the same conditions had a decay time of 16.6 ± 1.4 days. These values were found by averaging the coefficient from the least squares fit described previously. (See Figures 6 and 12.) The data for the ions ($Z > 2$) were taken from Figure 14 at $L = 3.25 \pm 1.0$ and $B = 0.20 \pm 0.03$ and the decay time had a value of 11.5 ± 1.0 days.

The loss processes that have been considered in the literature are pitch angle scattering and corrections to this from coulombic energy loss due to inelastic collisions with thermal electrons and charge-exchange with neutral hydrogen. The atmospheric interaction is generally just a boundary condition; that is, the particles mirroring above this boundary have no interaction and those mirroring below the boundary are lost from the system. The decay times observed by Injun V were for particles mirroring at low altitudes, so the interaction with the atmosphere must be considered quantitatively.

To check the hypothesis that the observed decay times are due to interaction with the atmosphere, it will be assumed that the loss process is due to inelastic coulomb collisions with both free and bound electrons. To obtain a relationship between decay time and the energy of the particle, the following equation given by Bethe (1964) is used.

$$-\frac{dE}{dt} = \frac{4\pi Z^2 e^4 \sqrt{m_i}}{\sqrt{2}\, m_e} \frac{\rho}{\sqrt{E}} \ln\left(\frac{4E\, m_e}{m_i} \times 10^5\right)$$

Where Z is the charge of the ion, m_i is the mass of the ion, m_e is the electron mass, and ρ is the density of electrons. For this order of magnitude calculation, the equation is rewritten in the

following form:

$$-\frac{\sqrt{2}\, m_e \sqrt{E}}{4 Z^2 e^4 \sqrt{m_i}\, \rho} \quad \frac{dE}{\ln\left(\frac{4E\, m_e}{m_i} \times 10^5\right)} = dt \ .$$

Both sides can now be integrated giving the time for a particle with energy $\bar{E}$ to lose enough energy such that it would no longer be detected. The energy $\bar{E}$ is found by evaluating the following integrals:

$$\frac{1}{e} \int_{E_1}^{\infty} \sqrt{E/E_*}\ e^{-\sqrt{E/E_*}}\ dE = \int_{\bar{E}}^{\infty} \sqrt{E/E_*}\ e^{-\sqrt{E/E_*}}\ dE$$

where E_1 is the lower energy limit of the passband. The upper limit is replaced by infinity with negligible error. The value of E_* is taken to be 0.0135 MeV for protons and 0.027 MeV for alpha particles. The value of $\bar{E}$ for protons is 0.516 MeV and for alpha particles is 1.696 MeV.

The time in days for a proton to lose this energy is then

$$T = \frac{7.442 \times 10^6}{\rho} \int_{0.304}^{0.516} \frac{\sqrt{E}\ dE}{\ln (217.9E)} \text{ days.}$$

This integral is evaluated by making a change of variables that transforms it into an exponential integral which is a tabulated function. Since the decay time of 30.3 days is known, the average density ρ can be determined. The above results give a value of $\rho = 7.41 \times 10^3$ electrons/cm^3.

The integral for the alpha particle decay time is

$$T = \frac{9.30 \times 10^5}{\rho} \int_{1.18}^{1.696} \frac{\sqrt{E}\, dE}{\ell n(54.5E)} \quad \text{days.}$$

Using the decay time of 16.6 days, the value of $\rho = 7.94 \times 10^3$ electrons/cm^3.

The orbit averaged atomic electron density is 6.31×10^3 electrons/cm^3. This was determined using the densities given by Cornwall et al. (1965) for a solar flux at 10.5 cm of 2×10^{-20} w/m^2 Hz. The orbit averaged free electron density is 6.9×10^2 electrons/cm^3 using the same model as Nakada and Mead (1965).

The above calculation was made only for the case of atomic electrons. To include the effects of the free electrons it is necessary to modify the logarithmic term in the above equation. This term represents the ratio of the maximum to the minimum transferences of energy. For scattering from free electrons, the value of logarithm is about 23.6 or about 5.3 times the bound case. This would then give an average density of $\rho = 9.97 \times 10^3$ electrons/cm^3.

This approximation does show that energy loss due to inelastic coulomb collisions with electrons should account for the observed decay times of energetic particle mirroring at low altitudes.

VI. CONCLUSIONS

The time histories of the intensities of trapped protons, alpha particles and ions ($Z > 2$) at low altitudes in the outer zone show marked variations. Increases in the intensity of trapped particles occur on the time scale of a day or two. The particle intensities decrease exponentially with characteristic decay times of 10 to 30 days. The particles with the higher value of Z decay more rapidly. Increases in the flux of trapped particles occur when there is a high flux of interplanetary particles and geomagnetic disturbances.

The alpha particle energy spectrum at $L = 3$, $B = 0.20$ has a shape similar to the proton energy spectra when compared on an energy per charge basis. Both differential energy spectra can be fit fairly well by an equation of the following form:

$$\frac{dJ}{dE} = K \sqrt{E/E_*} \exp\left(-\sqrt{E/E_*}\right)$$

where K is a normalizing constant and E_* is the characteristic energy. The polar cap proton and alpha particle spectra can also be fit by this same spectral form, but the two spectra have similar shapes in this case when a comparison is made on an energy per nucleon basis. The data from Explorer 35 fit the polar cap spectra,

indicating that the differential energy spectrum of solar protons (0.32 to 6.3 MeV) and the spectrum of solar alpha particles (2.0 to 10.2 MeV) are not changed when they arrive over the polar cap.

The source of increases in flux of trapped outer zone protons, alpha particles and ions ($Z > 2$) is thought to be from energetic low altitude polar cap particles. These particles are transported to lower L shells by a diffusive process involving fluctuating electric fields. This then gives rise to the charge dependent energy spectrum that is observed at $L = 3$. Though this is only a conjecture, it is more believable in the light of such evidence as shown in Figures 15 and 21, than just being the result of a change in the equatorial pitch angle distribution. This other possibility cannot be dismissed on the basis of the Injun V data. Hence, it will be necessary to wait until simultaneous observations are made at the equator and at low altitudes to see which conjecture is correct.

The losses of the observed low altitude outer zone particles seem to be explained by inelastic coulomb collision of the mirroring particles with free and bound electrons. Nothing can be said about the loss mechanisms that control the particles mirroring at higher altitudes from the Injun V observations, but the effects of the atmosphere decrease rapidly at higher altitudes and the longer decay time of 100 days is probably related to other mechanisms.

These observations seem to give a coherent picture of the low altitude magnetosphere but much more knowledge could be obtained from simultaneous observations by satellites in equatorial orbit with two other satellites, one in a low altitude polar orbit and one in interplanetary space. The complement of experiments should be able to observe the differential energy spectrum of protons, alpha particles and ions ($Z > 2$) over a much wider range of energies than the present observations. This information could be used to develop a detailed theory of magnetospheric processes.

ACKNOWLEDGEMENTS

This research was supported by the National Aeronautics and Space Administration under contract NAS1-8141 and by the U. S. Office of Naval Research contract N00014-68-A-0196-0003. The author was the recipient of a National Defense Education Act Title IV Graduate Fellowship and the Van Allen/Link Foundation Fellowship.

I would like to thank Professor James A. Van Allen for his encouragement. advice, and support in the research.

REFERENCES

Armstrong, T. P. and S. M. Krimigis, Statistical study of solar protons, alpha particles, and $Z \geq 3$ nuclei in 1967-1968, J. Geophys. Res., 76, 4230, 1971.

Bethe, H. A., Intermediate Quantum Mechanics, W. A. Benjamin, Inc., New York, 1964.

Birmingham, T. J., Convection electric fields and diffusion of trapped magnetospheric radiation, J. Geophys. Res., 74, 2169, 1969.

Cole, K. D., Rapid diffusion of energetic charged particles across magnetic fields, J. Geophys. Res., 76, 909, 1971.

Cornwall, J. M., A. R. Sims and R. S. White, Atmospheric Density experienced by radiation belt protons, J. Geophys. Res., 70, 3099, 1965.

Cornwall, J. M., Diffusion process influenced by conjugate-point wave phenomena, Radio Sci., 3, 740, 1968.

Cornwall, J. M., Radial diffusion of ionized helium and protons: A probe for magnetospheric dynamics, J. Geophys. Res., 77, 1756, 1972.

Davis, L., Jr. and D. G. Chang, On the effect of geomagnetic fluctuations on trapped particles, J. Geophys. Res., 67, 2169, 1962.

Davis, L. R. and J. M. Williamson, Low-energy trapped protons, Space Research, 3, 365, North Holland Publishing Co., 1963.

Evans, L. C. and E. C. Stone, Access of solar protons into the polar cap: A persistent north-south asymmetry, J. Geophys. Res., 74, 5127, 1969.

Fälthammar, C. -G., Effects of time-dependent electric fields on geomagnetically trapped radiation, J. Geophys. Res., 70, 2503, 1965.

Fälthammar, C. -G., Radial diffusion by violation of the third adiabatic invariant, in Earth's Particles and Fields, edited by B. M. McCormac, p. 157, Reinhold, New York, 1968.

REFERENCES (continued)

Fillius, R. W., Trapped protons in the inner radiation belt, J. Geophys. Res., 71, 97, 1966.

Frank, L. A., and H. D. Owens, Omnidirectional intensity contours of low-energy protons ($0.5 < E < 50$ keV) in the earth's outer radiation zone at the magnetic equator, J. Geophys. Res., 75, 1269, 1970.

Fritz, T. A., and S. M. Krimigis, Initial observations of geomagnetically trapped protons and alpha particles with OGO 4, J. Geophys. Res., 74, 5132, 1969.

Heckman, H. H., and A. H. Armstrong, Energy spectrum of geomagnetically trapped protons, J. Geophys. Res., 67, 1255, 1962.

Janni, J. F., Calculation of energy loss, range, path length, straggling, multiple scattering and the probability of inelastic nuclear collisions for 0.1 to 1000 MeV protons, AFWL-TR-65-150 of Air Force Weapons Laboratory, Kirtland Air Force Base, New Mexico, 1966.

Krimigis, S. M., and J. A. Van Allen, Geomagnetically trapped alpha particles, J. Geophys. Res., 72, 5779, 1967.

Krimigis, S. M., Alpha particles trapped in the earth's magnetic field in Particles and Fields in the Magnetosphere, edited by B. M. McCormac, D. Reidel, Dordrecht, Holland, 1970.

Krimigis, S. M., P. Verzariu, J. A. Van Allen, T. P. Armstrong, T. A. Fritz, and B. A. Randall, Trapped energetic nuclei $Z \geq 3$ in the earth's outer radiation zone, J. Geophys. Res., 75(22), 1970.

Lanzerotti, L. J., Access of solar particles to synchronous altitude, in Intercorrelated Satellite Observations Related to Solar Events, edited by V. Manno and D. E. Page, D. Reidel, Dordecht, Holland, 1970.

Lezniak, J. A. and W. R. Webber, Solar modulation of cosmic ray protons, helium nuclei, and electrons; a comparison of experiment with theory, J. Geophys. Res., 76, 1605, 1971.

REFERENCES (continued)

Mihalov, J. D., and R. S. White, Low-energy proton radiation belts, J. Geophys. Res., 71, 2207, 1966.

Nakada, M. P., and G. D. Mead, Diffusion of protons in the outer radiation belt, J. Geophys. Res., 70, 4777, 1965.

Paulikas, G. A., and J. B. Blake, Trapped alpha particles in the radiation belt, paper presented at the International Symposium on the Physics of the Magnetosphere, Washington, D. C., September 1968.

Paulakas, G. A., and J. B. Blake, Penetration of solar protons to synchronous altitude, J. Geophys. Res., 74, 2161, 1969.

Pizzella, G., Mechanism for the origin of the Van Allen belt, Univ. of Iowa Res. Rep. 70-9, 1970.

Pizzella, G., G. Knorr, and B. A. Randall, On the origin of the Van Allen protons, Univ. of Iowa Res. Rep. 70-10, 1970.

Pizzella, G., and L. A. Frank, Energy spectra for protons (200 eV < E < 1 MeV) intensities in the outer radiation zone, J. Geophys. Res., 76, 88, 1971.

Pizzella, G., and B. A. Randall, Differential energy spectrum of geomagnetically trapped protons with the Injun 5 satellite, J. Geophys. Res., 76, 2306, 1971.

Randall, B., Solid state detectors on Injun 5, Univ. of Iowa Res. Rep. 69-22, 1969.

Reid, G. C., and H. H. Sauer, Evidence for non-uniformity of solar-proton precipitation over the polar caps, J. Geophys. Res., 72, 4383, 1967.

Stevens, J. R., E. F. Martina and R. S. White, Proton energy distributions from 0.06 to 3.3 MeV at 6.6 earth radii, J. Geophys. Res., 75, 5373, 1970.

REFERENCES (continued)

Tverskoy, B. A., Transport and acceleration of charged particles in the earth's magnetosphere, Geomagnetism and Aeronomy, English Transl., 5, 617-628, 1965.

Van Allen, J. A., and N. F. Ness, Particle shadowing by the moon, J. Geophys. Res., 74, 71, 1969.

Van Allen, J. A., B. A. Randall, and S. M. Krimigis, Energetic C,N,O nuclei in the earth's outer radiation zone, J. Geophys. Res., 75, 6085, 1970.

Van Allen, J. A., and B. A. Randall, Evidence for direct, durable capture of 1- to 8-Mev solar alpha particles into geomagnetically trapped orbits, J. Geophys. Res., 76, 1830, 1971.

Van Allen, J. A., P. Venkatarangan and D. Venkatesan, Variability of the intensity ratios, proton/alphas, and alphas/medium nuclei during solar particle events, Univ. of Iowa Res. Rep. 71-26, 1971.

Whalen, B. A., J. R. Miller, and I. B. McDiarmid, Evidence for a solar-wind origin of auroral ions from low-energy ion measurements, J. Geophys. Res., 76, 2406, 1971.

FIGURE CAPTIONS

Figure 1. An assembly drawing showing the collimator of the Injun V Proton-Electron Telescope Detectors and a graph of the particle penetration depth as a function of angle.

Figure 2. ΔE vs E curves for protons incident on the PET detectors with a 0.17 cm^{-2} nickel foil in front.

Figure 3. An assembly drawing showing the collimator of the Injun V alpha particle detector and a graph of the particle penetration depth as a function of angle.

Figure 4. ΔE vs E curves for protons, alpha particles, and carbon and oxygen ions incident on an 8.5 micron silicon detector with a 0.36 mg cm^{-2} nickel foil in front (Van Allen et al., 1970).

Figure 5. ΔE vs E curves for protons, alpha particles and ions ($Z > 2$) incident on the Explorer 35 solid state detector (Van Allen et al., 1971).

Figure 6. A plot of detector counting rate as a function of time for trapped protons at $L = 3$ and interplanetary protons.

Figure 7. A plot of detector counting rate for interplanetary alpha particles and geomagnetic index A_p as a function of time.

FIGURE CAPTIONS (continued)

Figure 8. A plot of detector counting rate for interplanetary ions ($Z > 2$) as a function of time.

Figure 9. A plot of detector counting rate for alpha particles as a function of time for $L = 6.6$.

Figure 10. A plot of detector counting rate for alpha particles as a function of time for $L = 4$.

Figure 11. A plot of detector counting rate for alpha particles as a function of time for $L = 3.5$.

Figure 12. A plot of detector counting rate for alpha particles as a function of time for $L = 3$.

Figure 13. A plot of detector counting rate for alpha particles as a function of time for $L = 2.5$.

Figure 14. A plot of detector counting rate for alpha particles and ions ($Z > 2$) as a function of time for $L = 3.25 \pm 1.0$.

Figure 15. Detector counting rates for electrons, protons and alpha particles for two polar cap passes with comparative data from Explorer 35.

Figure 16. The alpha particle to proton intensity ratio for 0.3 MeV per nucleon particles at $L = 3$ as a function of time.

Figure 17. The ion ($Z > 2$) to alpha particle intensity ratio for 0.3 MeV per nucleon particles at $L = 3.25$ as a function of time.

FIGURE CAPTIONS (continued)

Figure 18. Eight different integral proton spectra at L = 3 normalized to the integral of Pizzella's differential spectral form.

Figure 19. Four different integral polar cap proton spectra normalized to the integral of Pizzella's differential spectral form.

Figure 20. Three different integral polar cap proton spectra and four integral spectra at L = 3 normalized to the integral of Pizzella's differential spectral form.

Figure 21. A plot of the trans-L motion of proton disturbances in units of $hours^{-1}$ as a function of L. The straight-line fit is given by $\Delta L/\Delta t = 5.85 \times 10^{-4} L^{3.23}$ (L/hour).

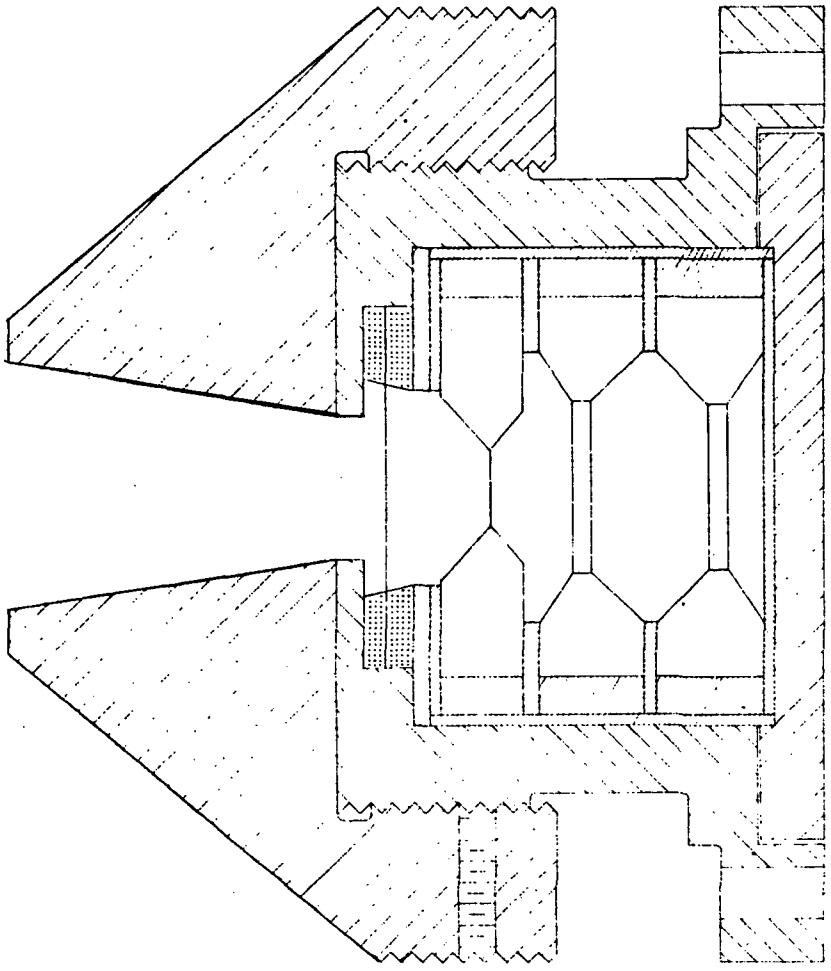

D-GE8-1145

PARTICLE PENETRATION DEPTH
VS. ANGLE
FOR INJUN V
PET APERTURE

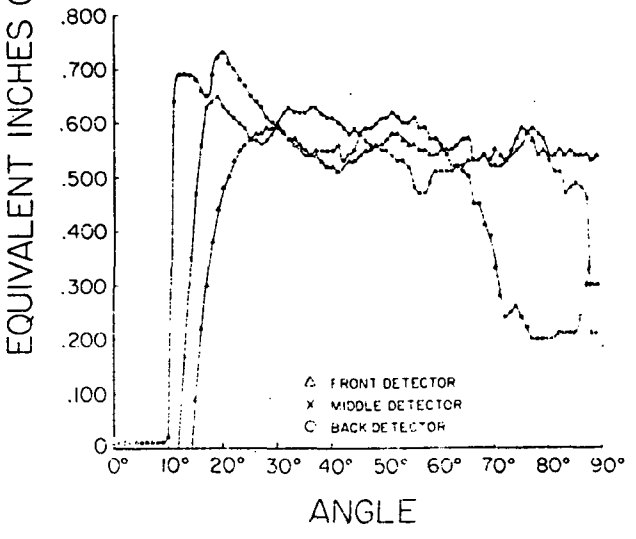

Figure 1

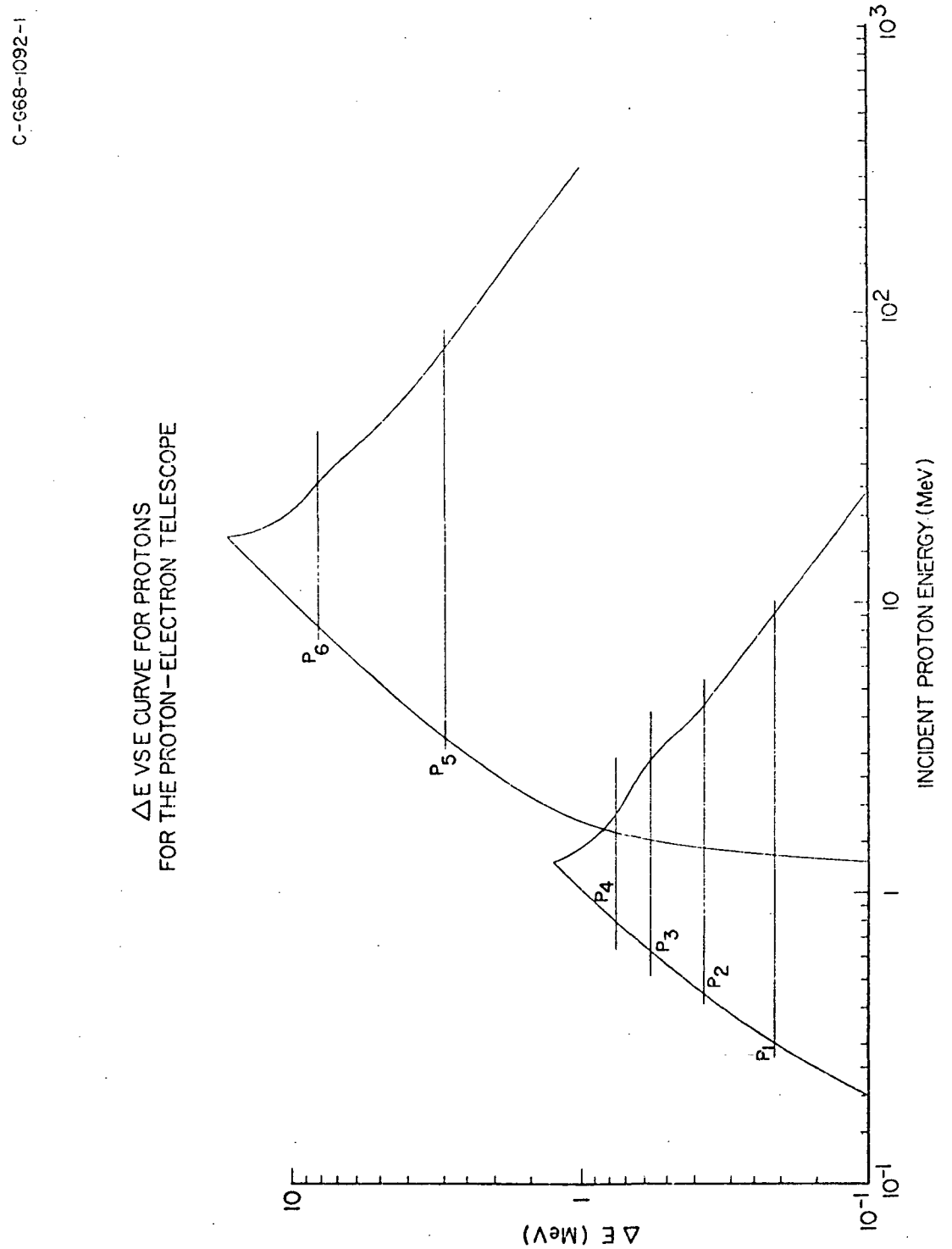
C-668-1092-1
ΔE VSE CURVE FOR PROTONS
FOR THE PROTON–ELECTRON TELESCOPE
ΔE (MeV)
10
1
10^{-1}
10^{-1}
1
10
10^2
10^3
INCIDENT PROTON ENERGY (MeV)
P6
P5
P4
P3
P2
P1

Figure 2

C-G68-1142

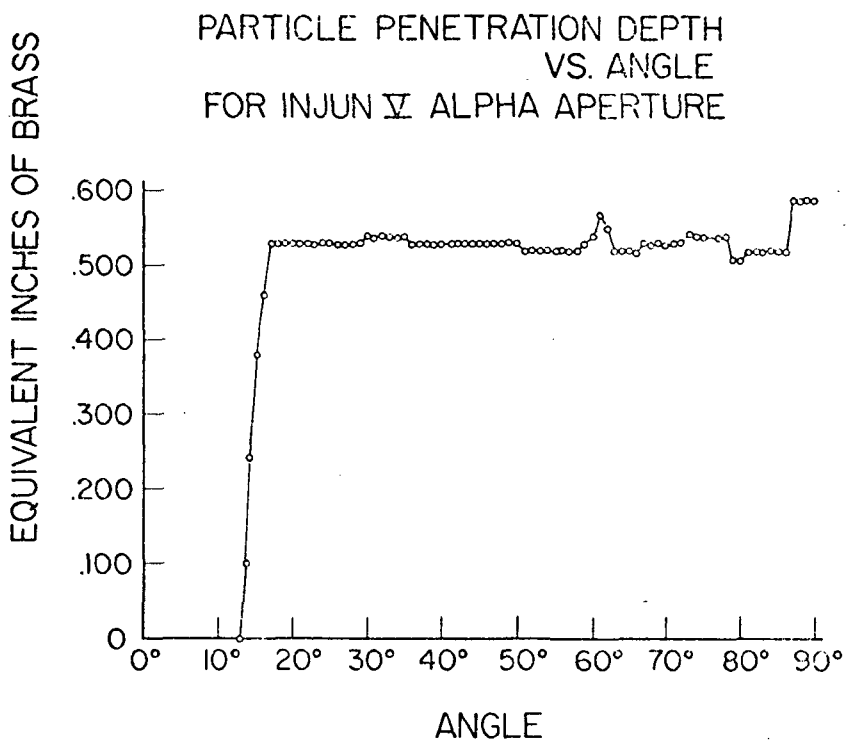

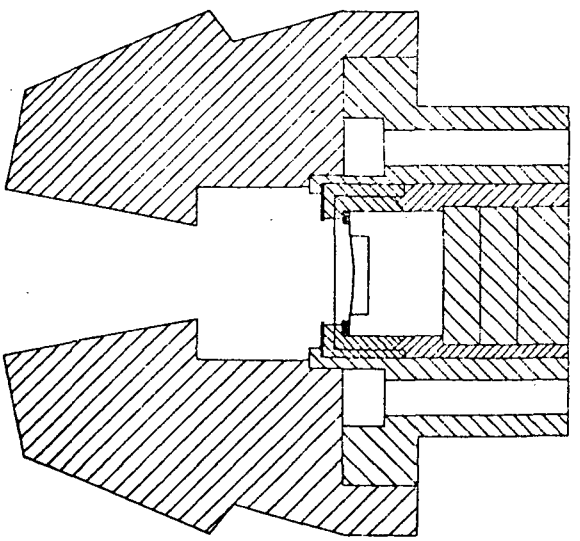

Figure 3

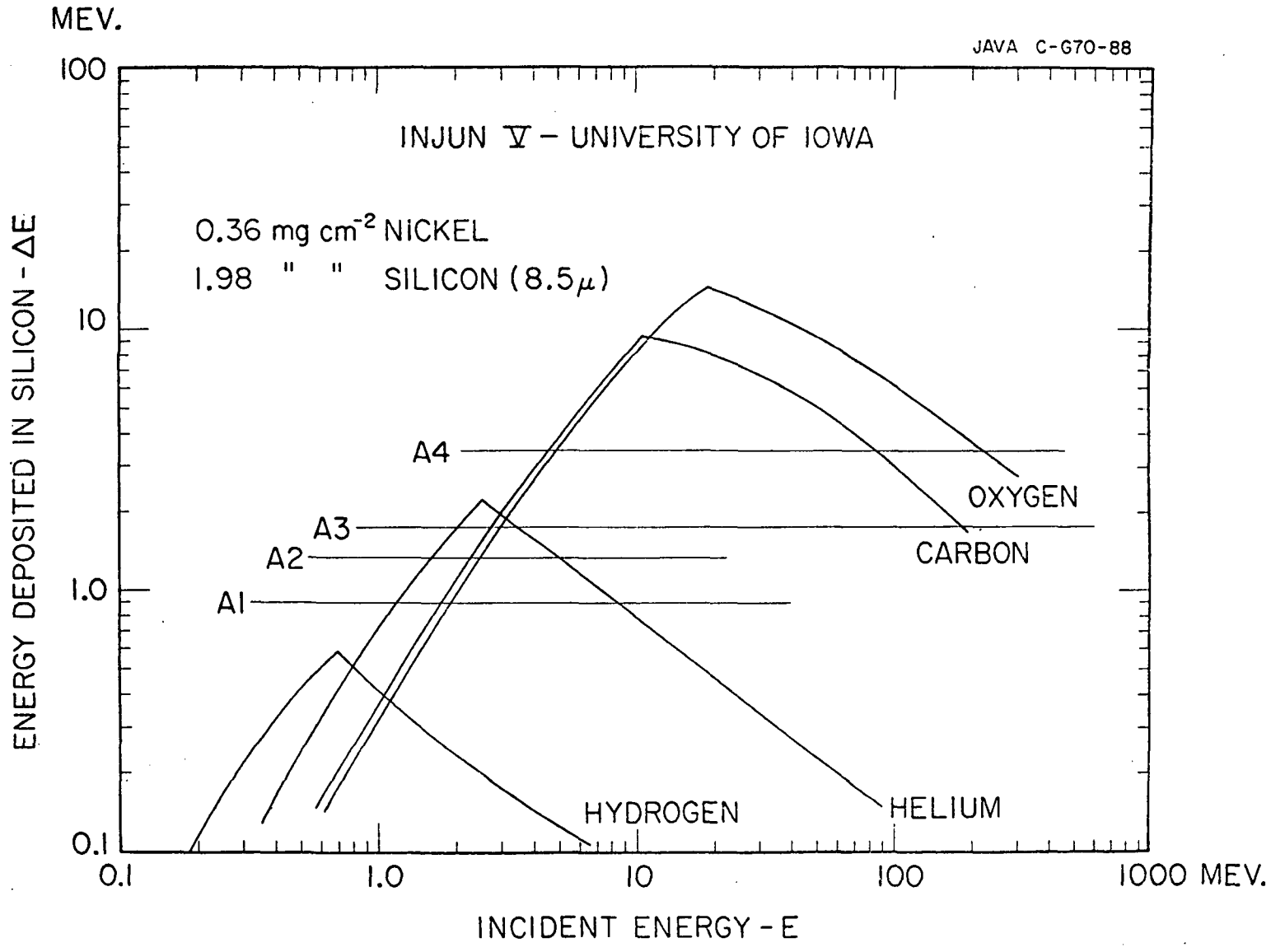
MEV.
JAVA C-G70-88
100
INJUN V – UNIVERSITY OF IOWA
0.36 mg cm⁻² NICKEL
1.98 " " SILICON (8.5μ)
10
A4
OXYGEN
A3
A2
CARBON
1.0
A1
HYDROGEN
HELIUM
0.1
ENERGY DEPOSITED IN SILICON - ΔE
0.1
1.0
10
100
1000 MEV.
INCIDENT ENERGY - E

Figure 4

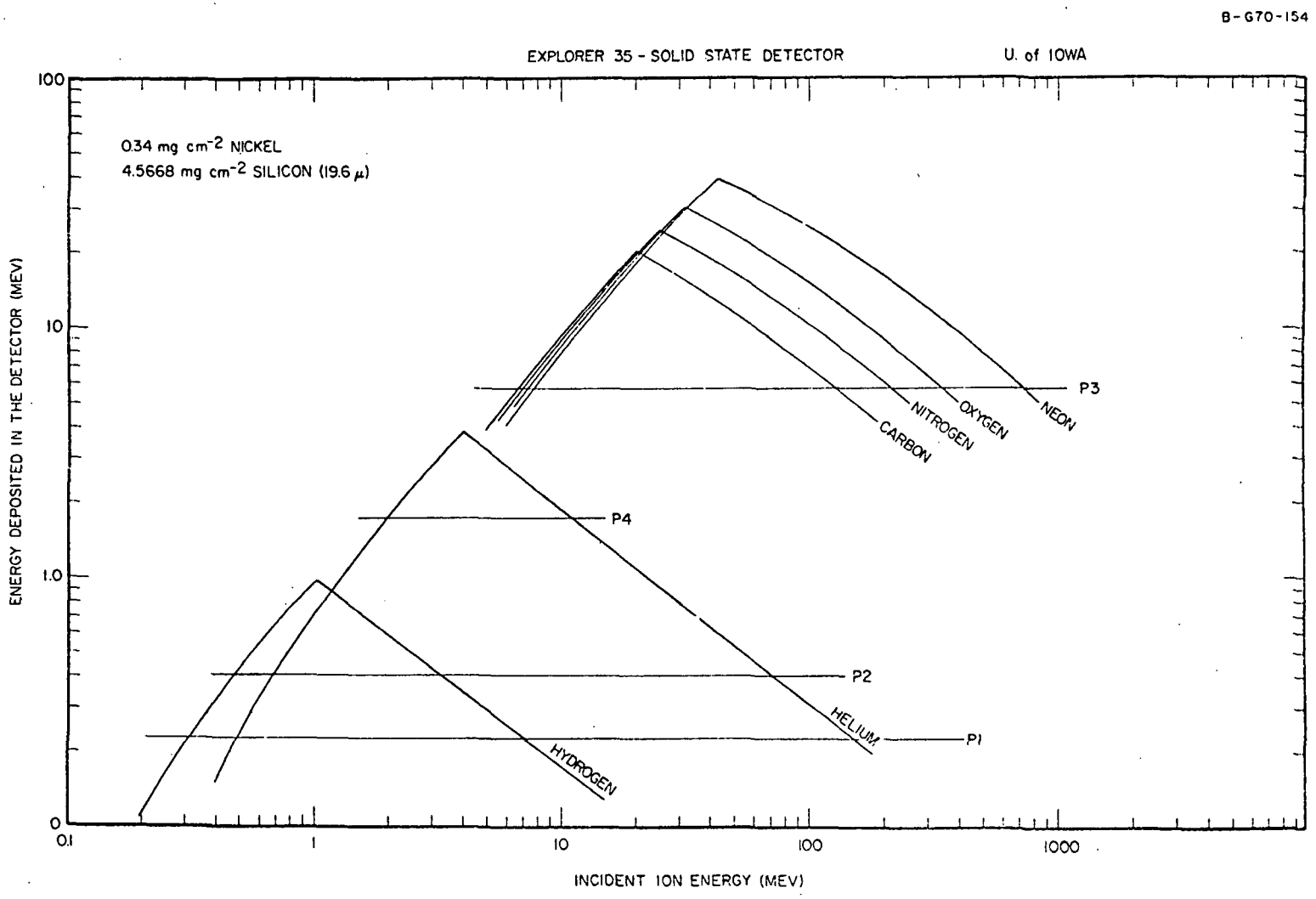
B-G70-154
EXPLORER 35 - SOLID STATE DETECTOR
U. of IOWA
0.34 mg cm-2 NICKEL
4.5668 mg cm-2 SILICON (19.6 μ)
ENERGY DEPOSITED IN THE DETECTOR (MEV)
INCIDENT ION ENERGY (MEV)
100
10
1.0
0
0.1
1
10
100
1000
P3
P4
P2
P1
NEON
OXYGEN
NITROGEN
CARBON
HELIUM
HYDROGEN

Figure 5

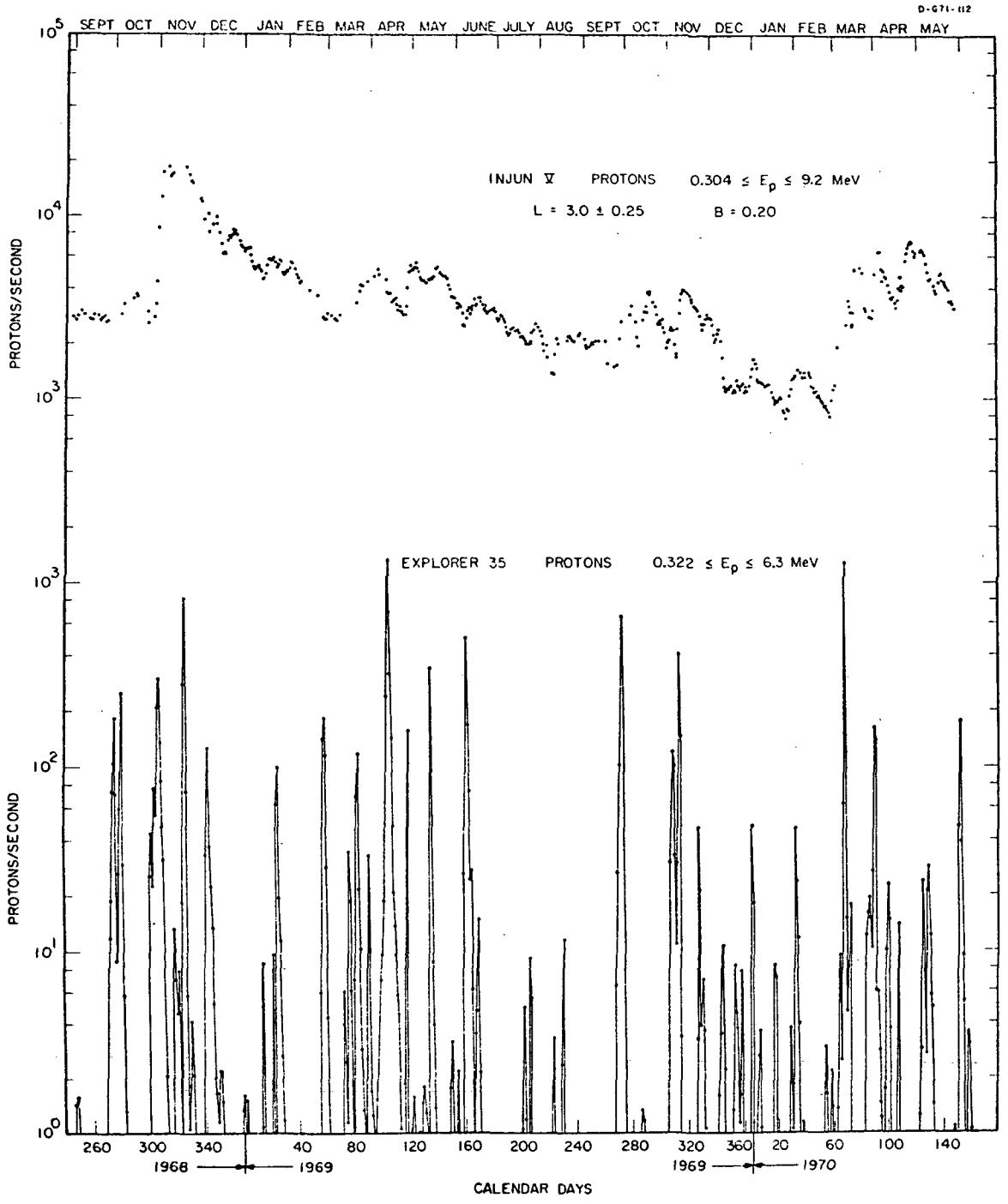
D-G71-112
SEPT OCT NOV DEC JAN FEB MAR APR MAY JUNE JULY AUG SEPT OCT NOV DEC JAN FEB MAR APR MAY
INJUN V PROTONS 0.304 ≤ Ep ≤ 9.2 MeV
L = 3.0 ± 0.25 B = 0.20
EXPLORER 35 PROTONS 0.322 ≤ Ep ≤ 6.3 MeV
PROTONS/SECOND
PROTONS/SECOND
CALENDAR DAYS
1968
1969
1969
1970

Figure 6

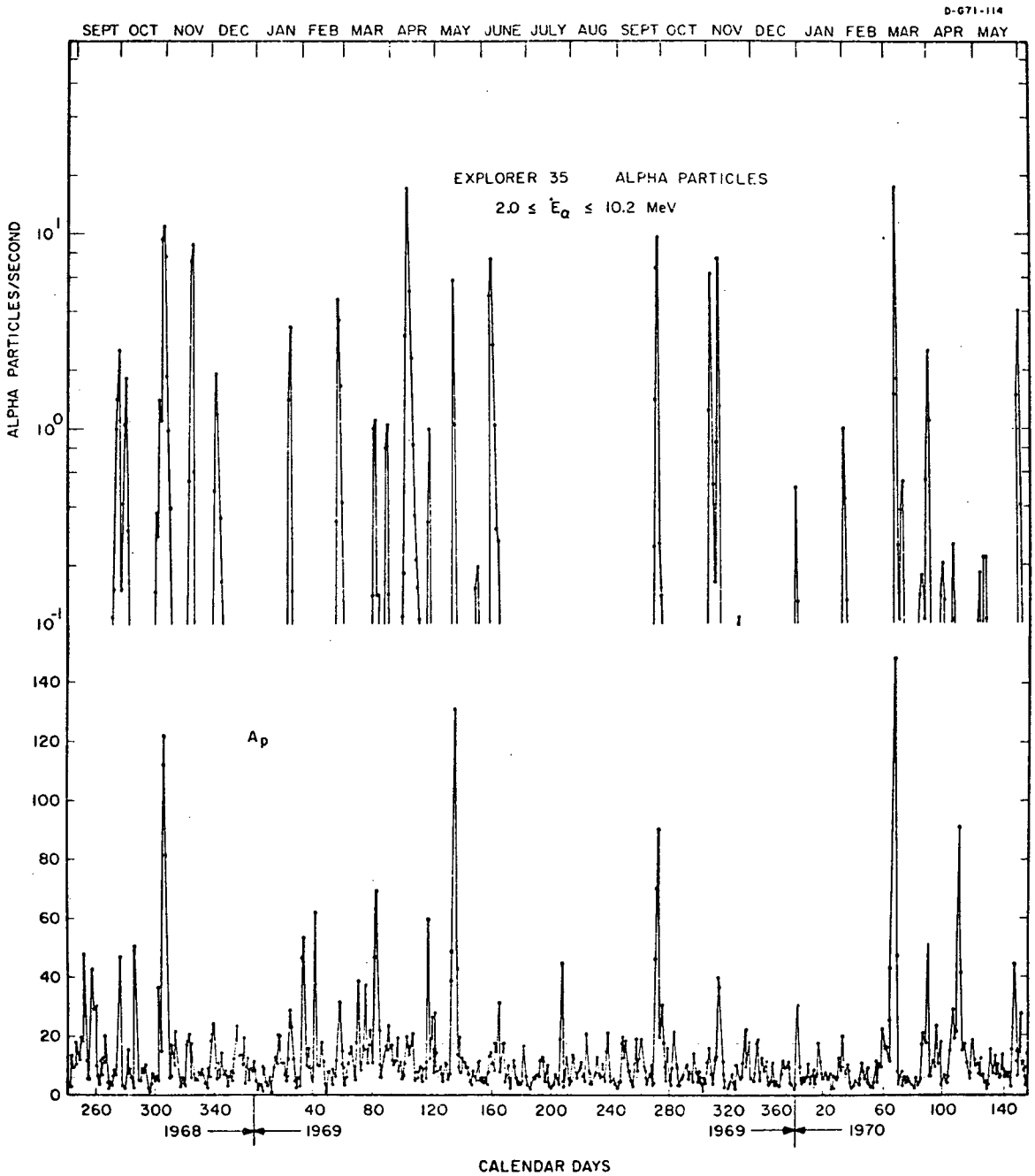
D-G71-114
SEPT OCT NOV DEC JAN FEB MAR APR MAY JUNE JULY AUG SEPT OCT NOV DEC JAN FEB MAR APR MAY
EXPLORER 35 ALPHA PARTICLES
2.0 ≤ Eα ≤ 10.2 MeV
ALPHA PARTICLES/SECOND
10^1
10^0
10^-1
Ap
0
20
40
60
80
100
120
140
260 300 340 40 80 120 160 200 240 280 320 360 20 60 100 140
1968 1969 1969 1970
CALENDAR DAYS

Figure 7

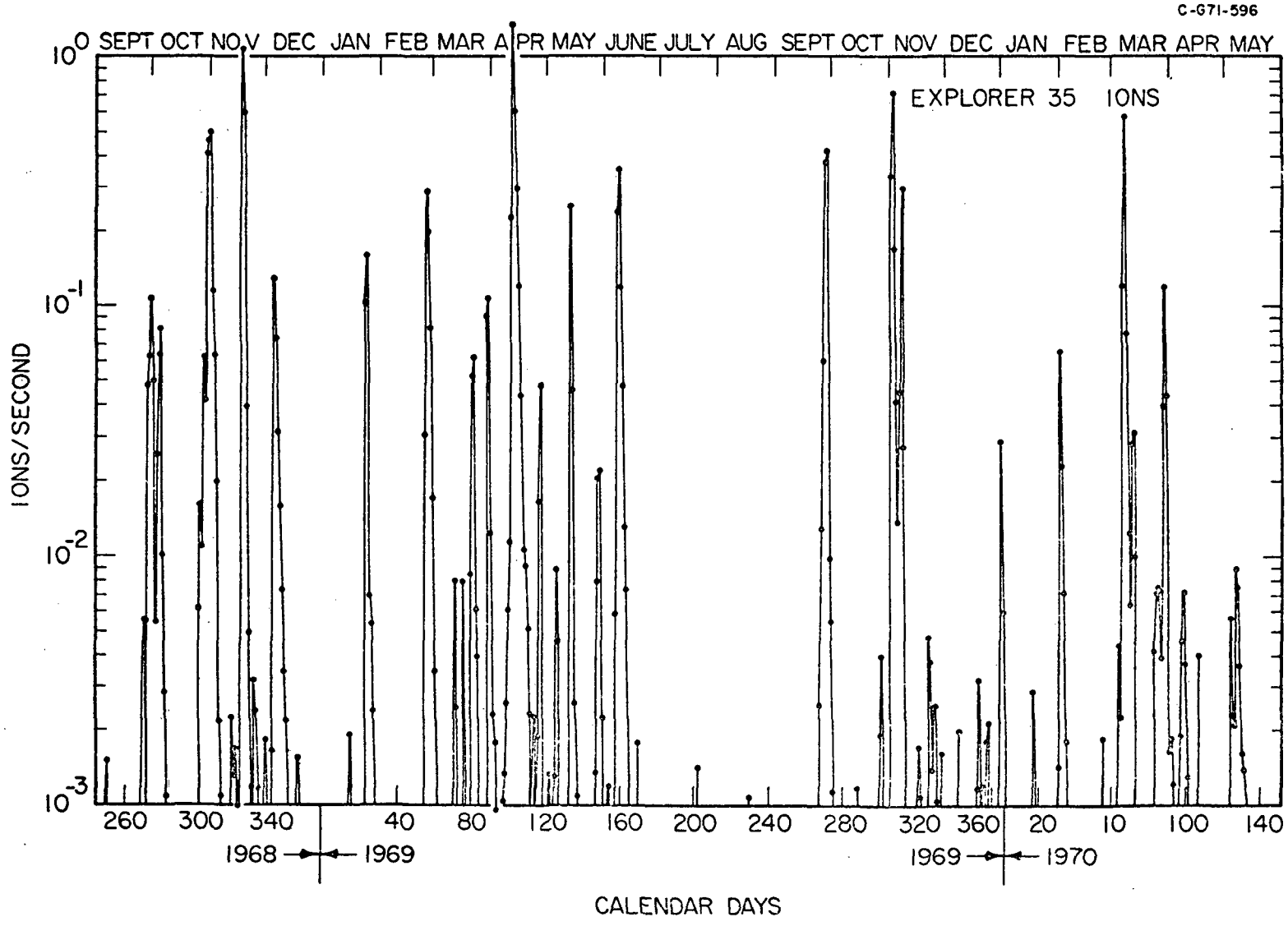
C-G71-596
SEPT OCT NOV DEC JAN FEB MAR APR MAY JUNE JULY AUG SEPT OCT NOV DEC JAN FEB MAR APR MAY
EXPLORER 35 IONS
IONS/SECOND
10^{0}
10^{-1}
10^{-2}
10^{-3}
260 300 340 40 80 120 160 200 240 280 320 360 20 10 100 140
1968 → ← 1969
1969 → ← 1970
CALENDAR DAYS

Figure 8

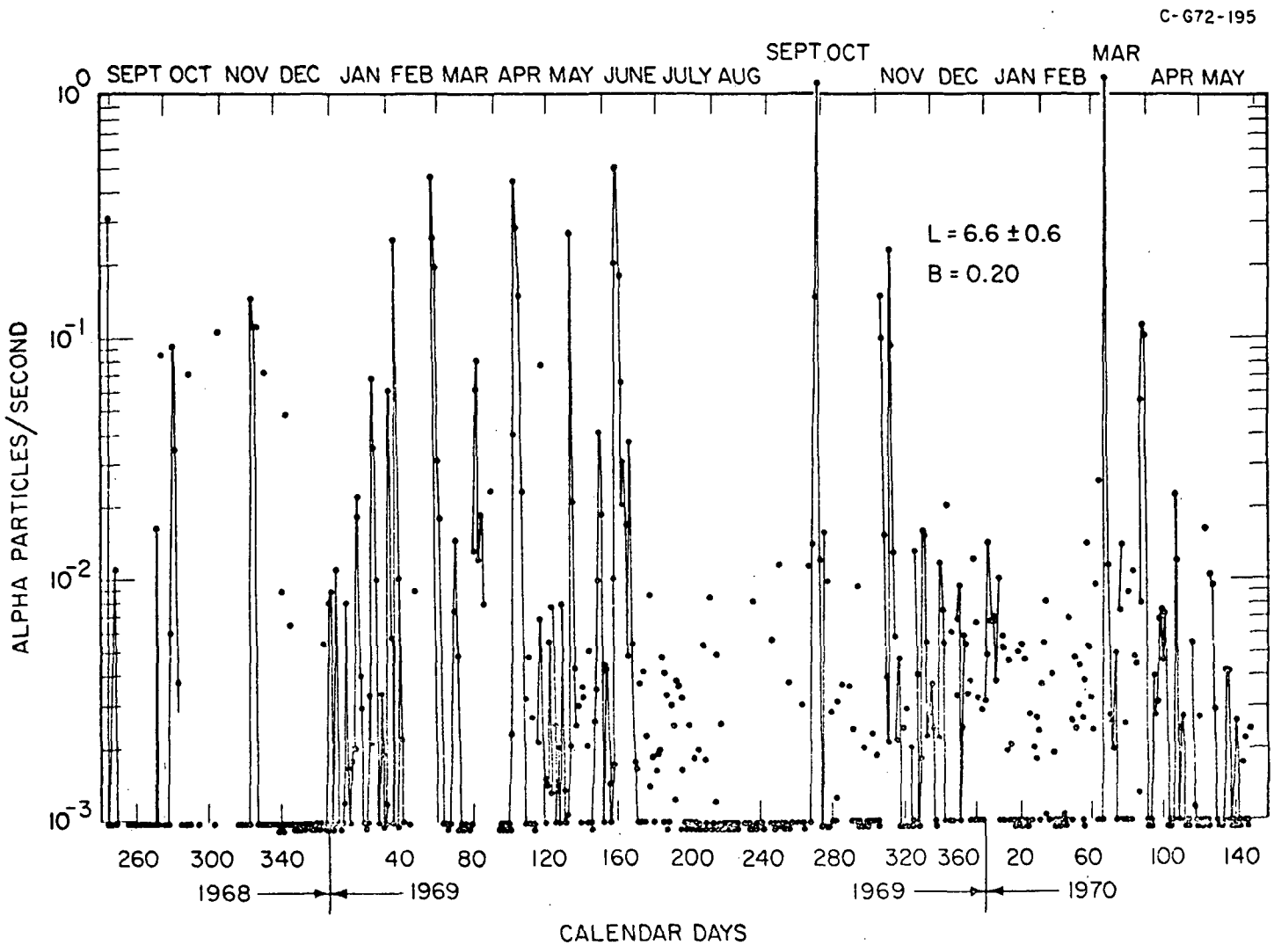
C-G72-195
SEPT OCT NOV DEC JAN FEB MAR APR MAY JUNE JULY AUG
SEPT OCT
NOV DEC JAN FEB
MAR
APR MAY
L = 6.6 ± 0.6
B = 0.20
ALPHA PARTICLES/SECOND
10^{0}
10^{-1}
10^{-2}
10^{-3}
260 300 340 40 80 120 160 200 240 280 320 360 20 60 100 140
1968
1969
1969
1970
CALENDAR DAYS

Figure 9

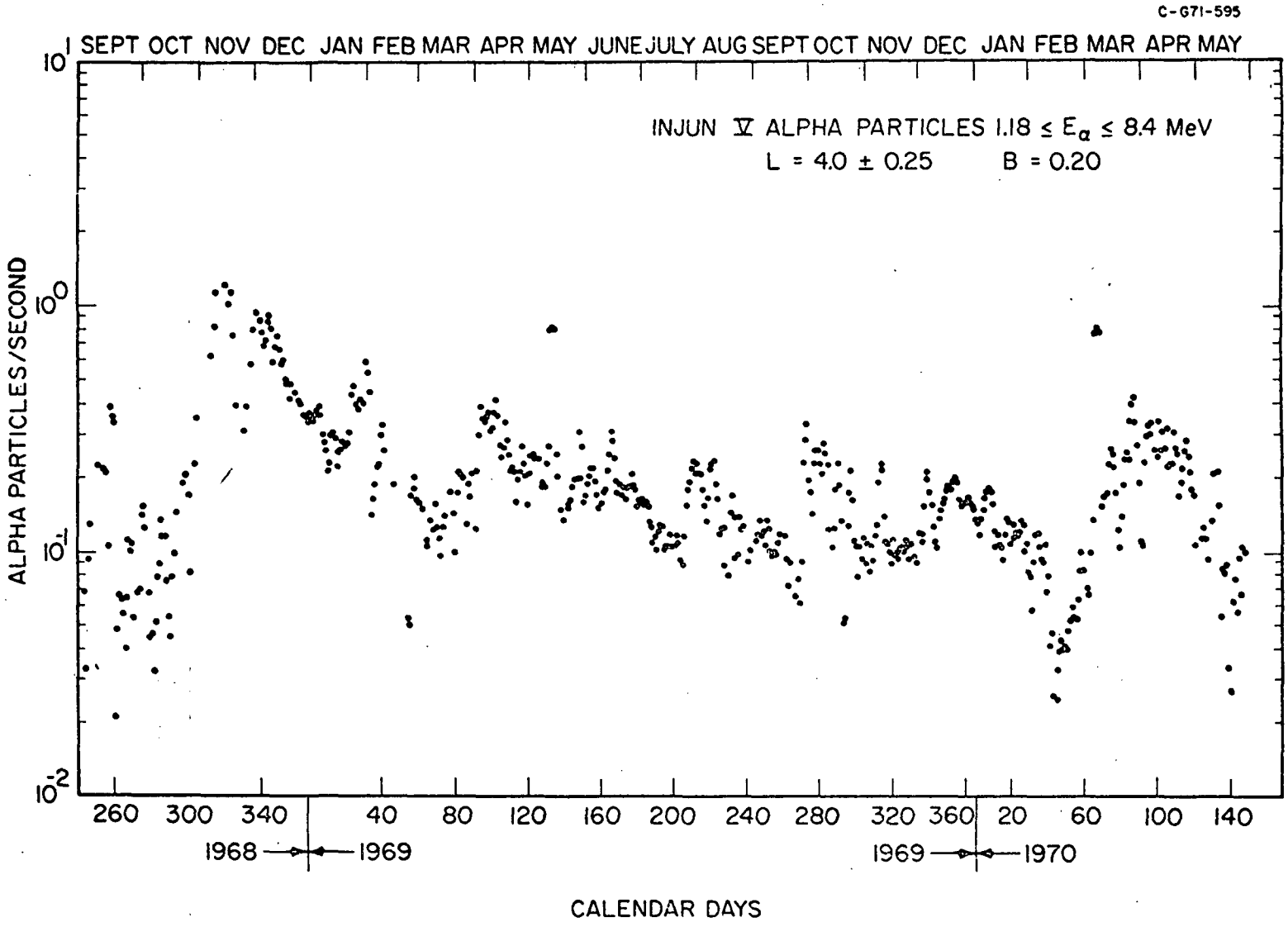
C-G71-595
SEPT OCT NOV DEC JAN FEB MAR APR MAY JUNE JULY AUG SEPT OCT NOV DEC JAN FEB MAR APR MAY
INJUN V ALPHA PARTICLES 1.18 ≤ Eα ≤ 8.4 MeV
L = 4.0 ± 0.25 B = 0.20
ALPHA PARTICLES/SECOND
10
10^0
10^-1
10^-2
260 300 340 40 80 120 160 200 240 280 320 360 20 60 100 140
1968 1969 1969 1970
CALENDAR DAYS

Figure 10

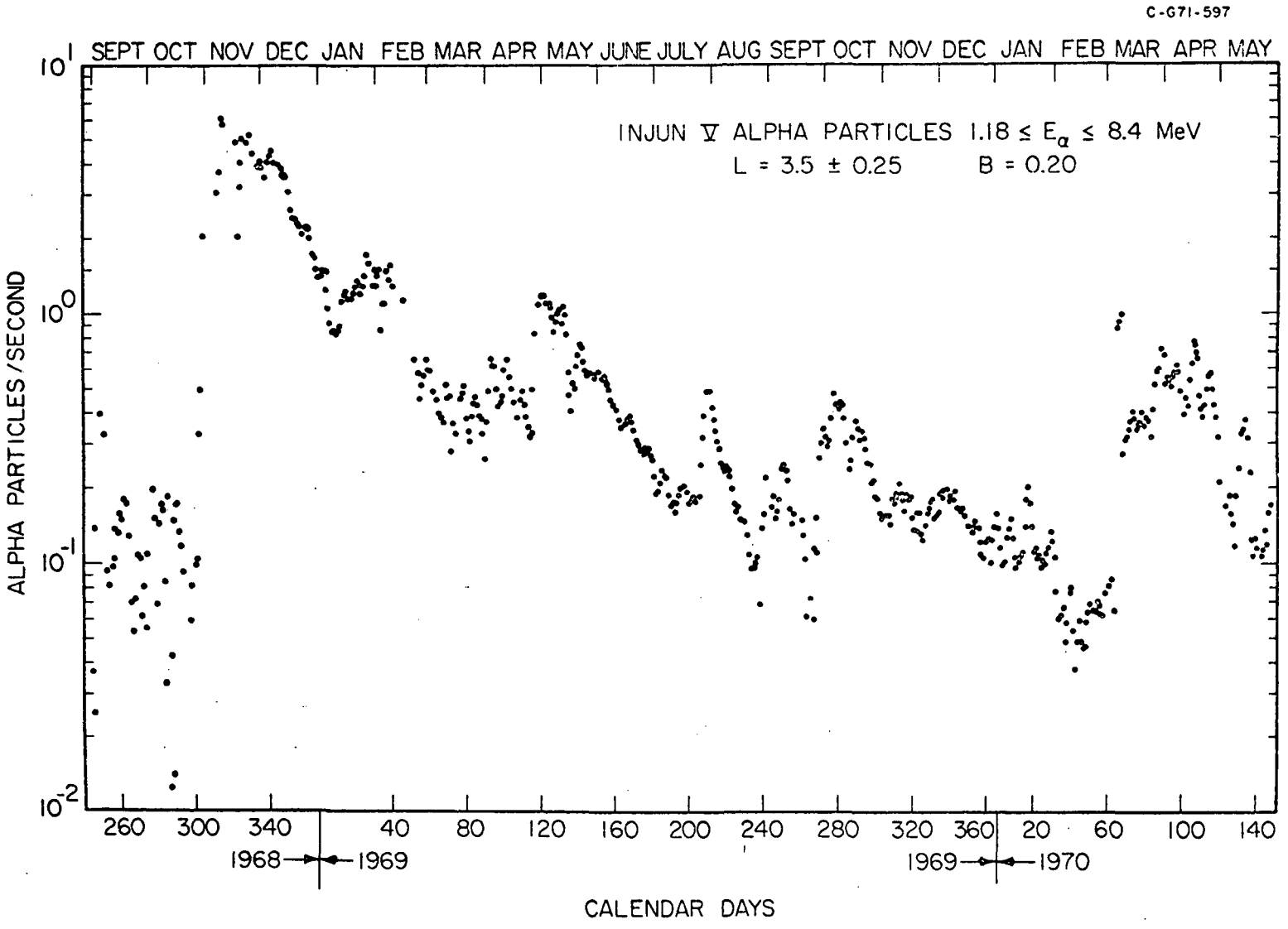
C-G71-597
SEPT OCT NOV DEC JAN FEB MAR APR MAY JUNE JULY AUG SEPT OCT NOV DEC JAN FEB MAR APR MAY
INJUN V ALPHA PARTICLES 1.18 ≤ Eα ≤ 8.4 MeV
L = 3.5 ± 0.25 B = 0.20
ALPHA PARTICLES/SECOND
10^1
10^0
10^-1
10^-2
260 300 340 40 80 120 160 200 240 280 320 360 20 60 100 140
1968 1969
1969 1970
CALENDAR DAYS

Figure 11

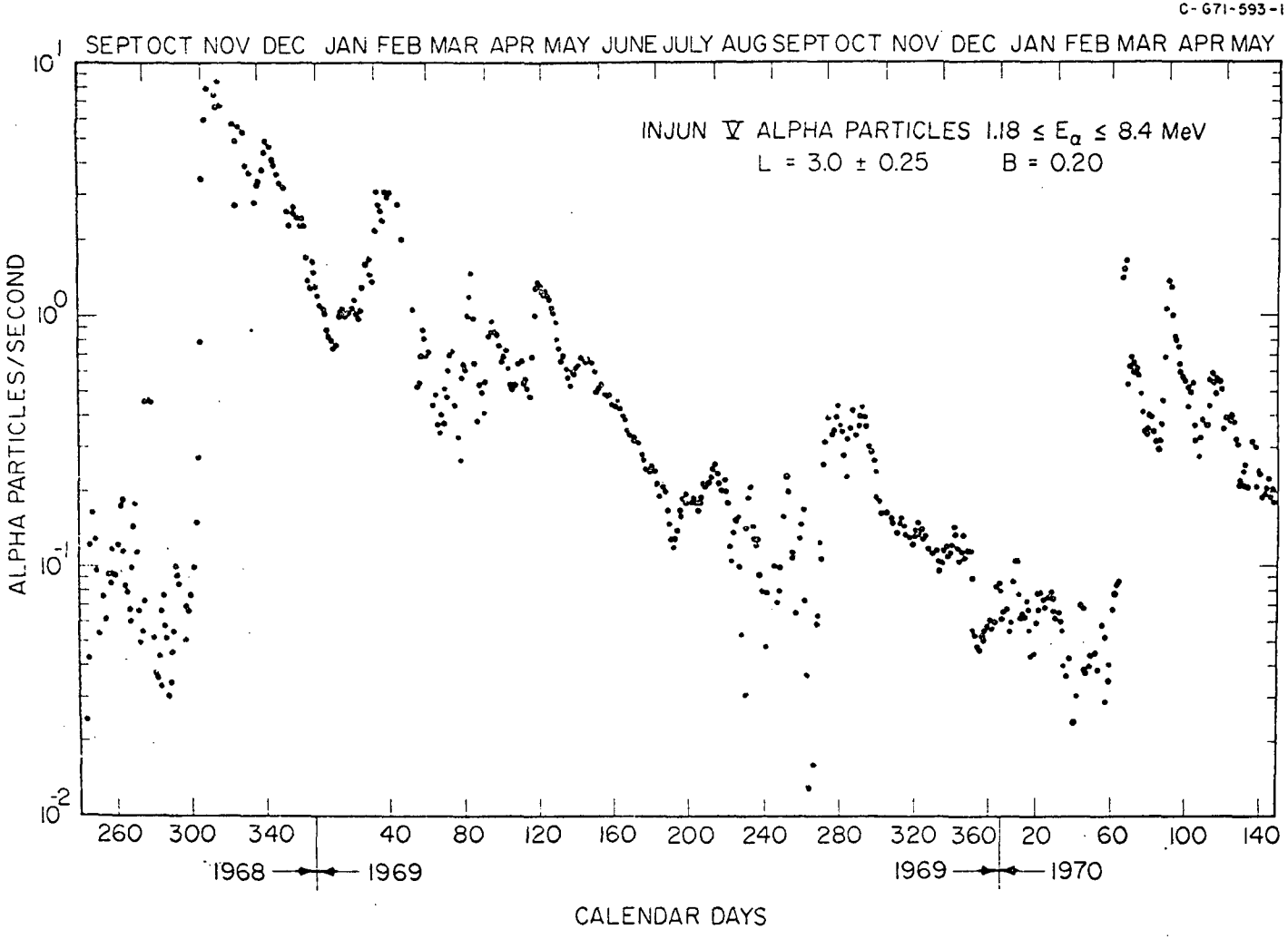
C-G71-593-1
SEPT OCT NOV DEC JAN FEB MAR APR MAY JUNE JULY AUG SEPT OCT NOV DEC JAN FEB MAR APR MAY
INJUN V ALPHA PARTICLES 1.18 ≤ Eα ≤ 8.4 MeV
L = 3.0 ± 0.25 B = 0.20
ALPHA PARTICLES/SECOND
10^1
10^0
10^-1
10^-2
260 300 340 40 80 120 160 200 240 280 320 360 20 60 100 140
1968 1969 1969 1970
CALENDAR DAYS

Figure 12

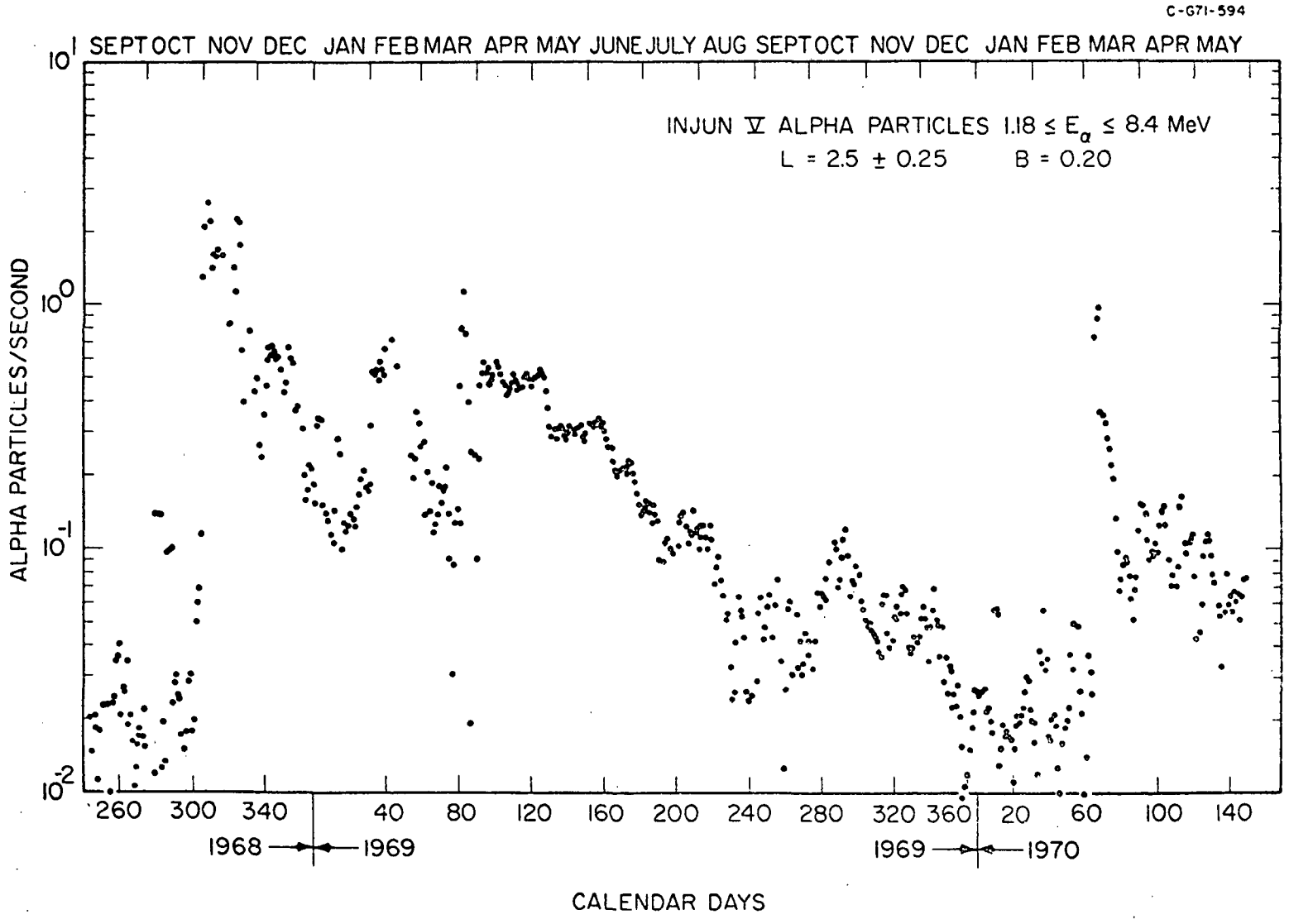
C-G71-594
SEPT OCT NOV DEC JAN FEB MAR APR MAY JUNE JULY AUG SEPT OCT NOV DEC JAN FEB MAR APR MAY
INJUN V ALPHA PARTICLES 1.18 ≤ Eα ≤ 8.4 MeV
L = 2.5 ± 0.25 B = 0.20
ALPHA PARTICLES/SECOND
10^1
10^0
10^-1
10^-2
260 300 340 40 80 120 160 200 240 280 320 360 20 60 100 140
1968 1969 1969 1970
CALENDAR DAYS

Figure 13

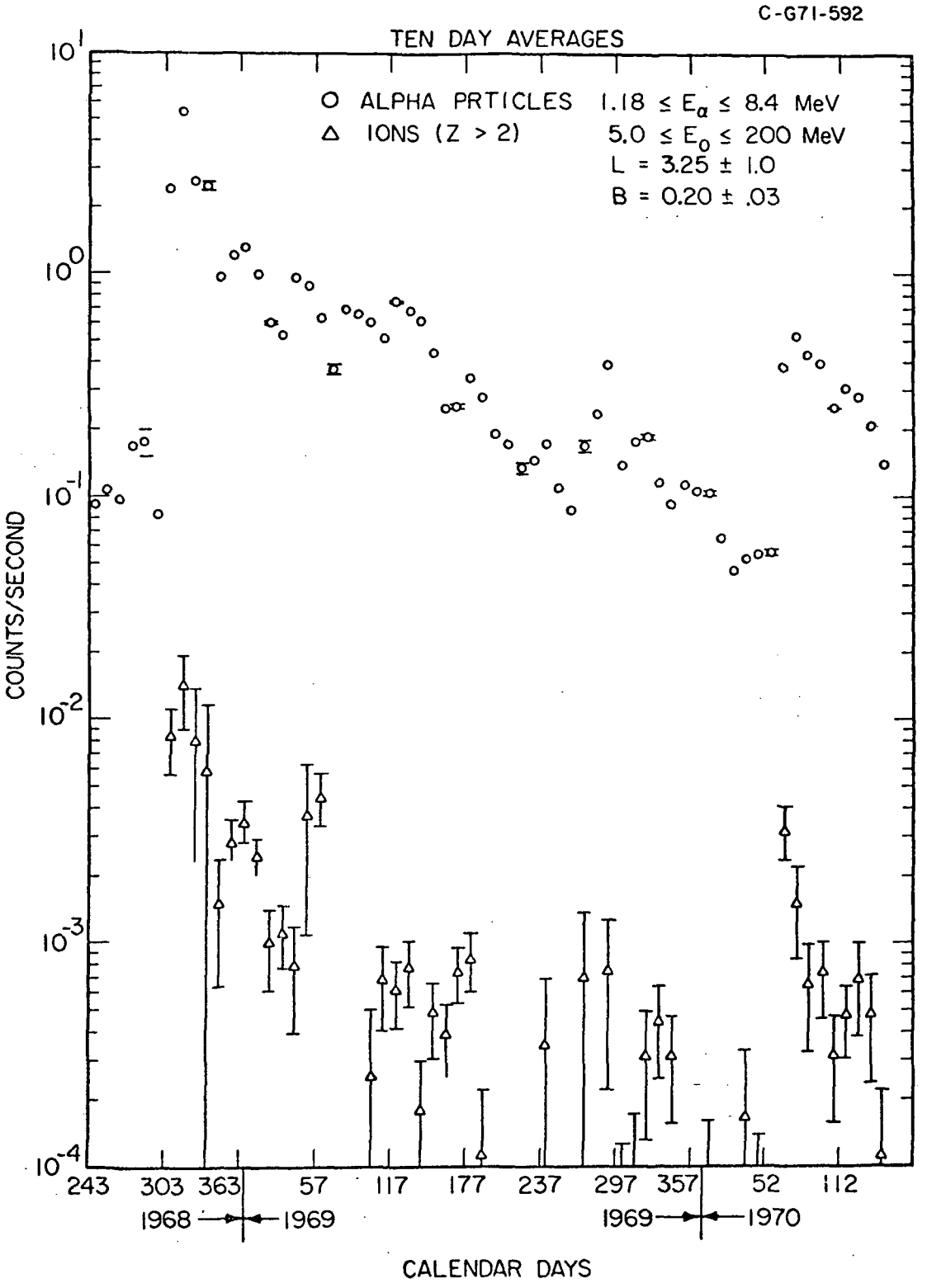
C-G71-592
TEN DAY AVERAGES
O ALPHA PRTICLES 1.18 ≤ E_α ≤ 8.4 MeV
Δ IONS (Z > 2) 5.0 ≤ E_0 ≤ 200 MeV
L = 3.25 ± 1.0
B = 0.20 ± .03
COUNTS/SECOND
10^{1}
10^{0}
10^{-1}
10^{-2}
10^{-3}
10^{-4}
243 303 363 57 117 177 237 297 357 52 112
1968 1969 1969 1970
CALENDAR DAYS

Figure 14

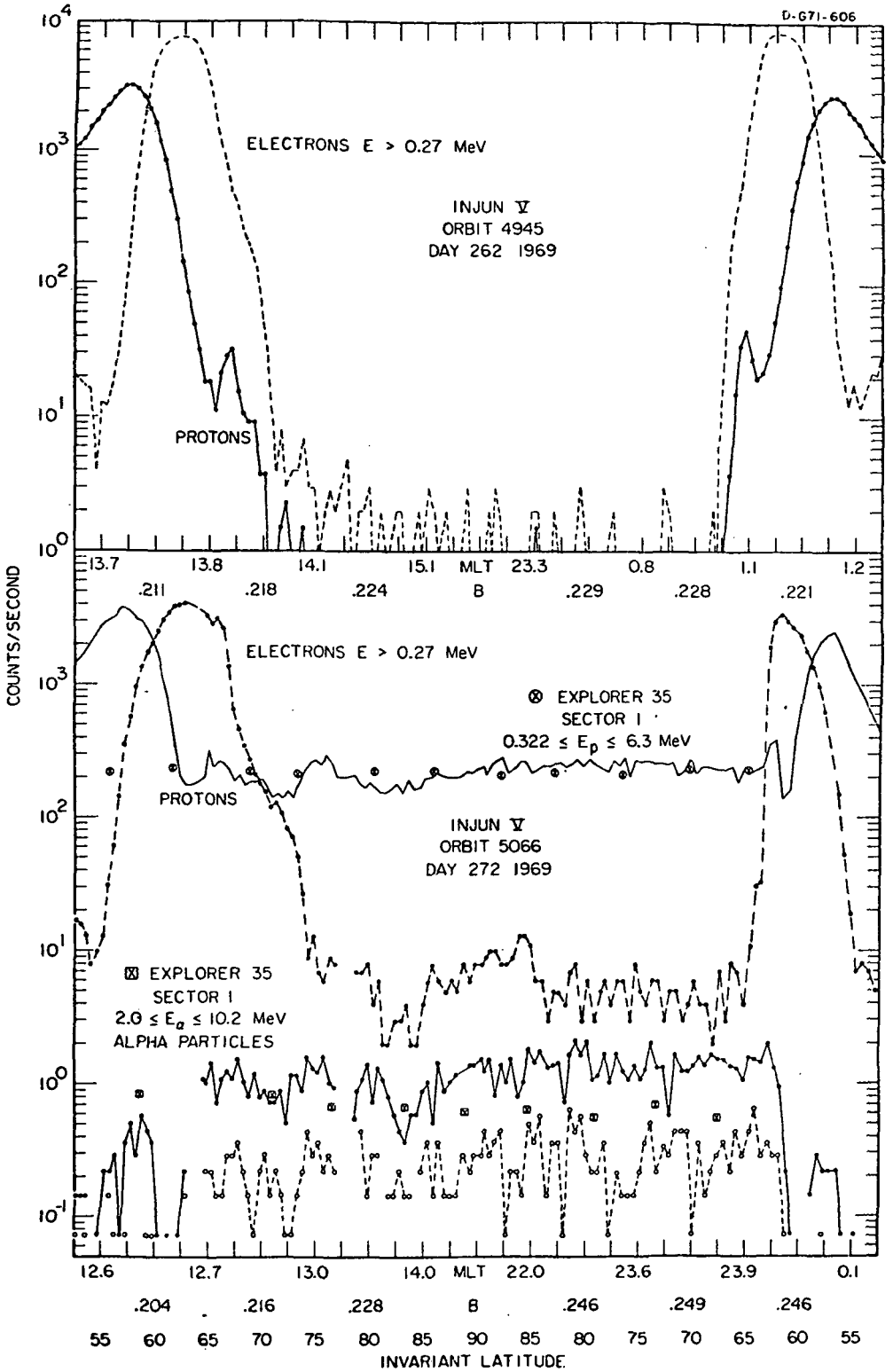
D-671-606
ELECTRONS E > 0.27 MeV
INJUN V
ORBIT 4945
DAY 262 1969
PROTONS
13.7 13.8 14.1 15.1 MLT 23.3 0.8 1.1 1.2
.211 .218 .224 B .229 .228 .221
ELECTRONS E > 0.27 MeV
EXPLORER 35
SECTOR I
0.322 ≤ Ep ≤ 6.3 MeV
PROTONS
INJUN V
ORBIT 5066
DAY 272 1969
EXPLORER 35
SECTOR I
2.0 ≤ Eα ≤ 10.2 MeV
ALPHA PARTICLES
COUNTS/SECOND
12.6 12.7 13.0 14.0 MLT 22.0 23.6 23.9 0.1
.204 .216 .228 B .246 .249 .246
55 60 65 70 75 80 85 90 85 80 75 70 65 60 55
INVARIANT LATITUDE

Figure 15

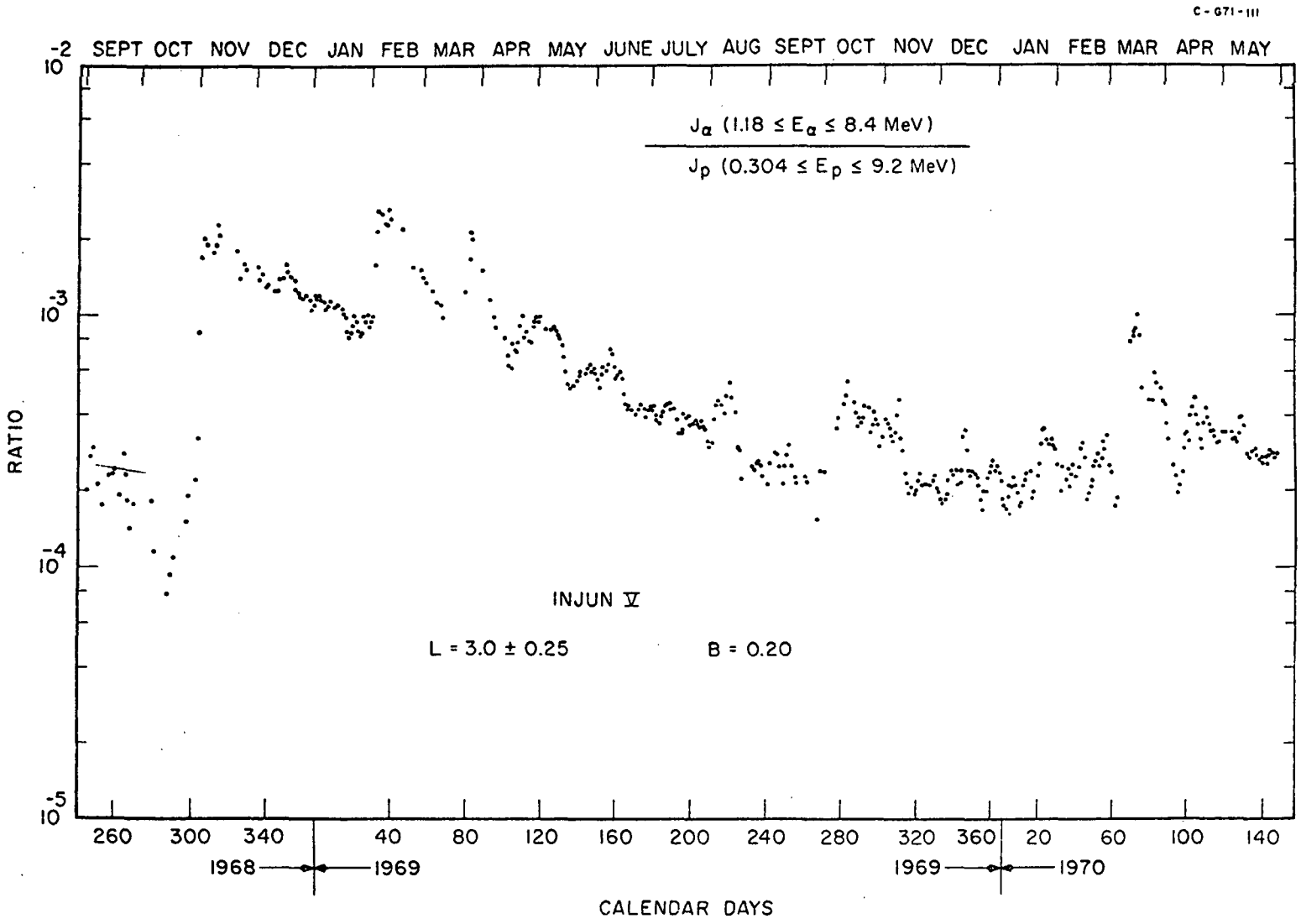
C-671-111
-2 SEPT OCT NOV DEC JAN FEB MAR APR MAY JUNE JULY AUG SEPT OCT NOV DEC JAN FEB MAR APR MAY
10^{-2}
10^{-3}
10^{-4}
10^{-5}
RATIO
J_α (1.18 ≤ E_α ≤ 8.4 MeV)
J_p (0.304 ≤ E_p ≤ 9.2 MeV)
INJUN V
L = 3.0 ± 0.25
B = 0.20
260 300 340 40 80 120 160 200 240 280 320 360 20 60 100 140
1968
1969
1969
1970
CALENDAR DAYS

Figure 16

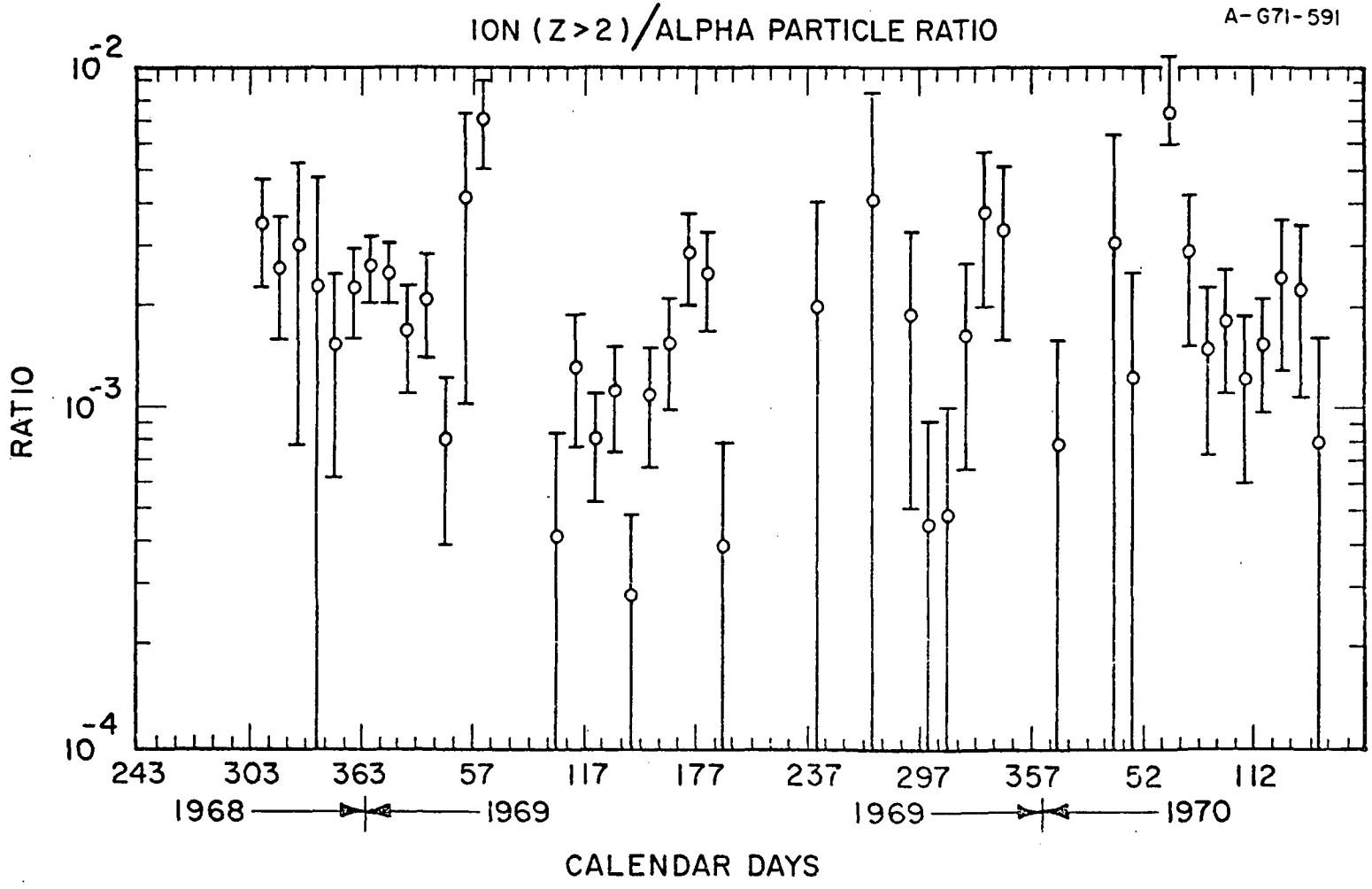
ION (Z>2)/ALPHA PARTICLE RATIO
A-G71-591
RATIO
10^{-2}
10^{-3}
10^{-4}
243
303
363
57
117
177
237
297
357
52
112
1968
1969
1969
1970
CALENDAR DAYS

Figure 17

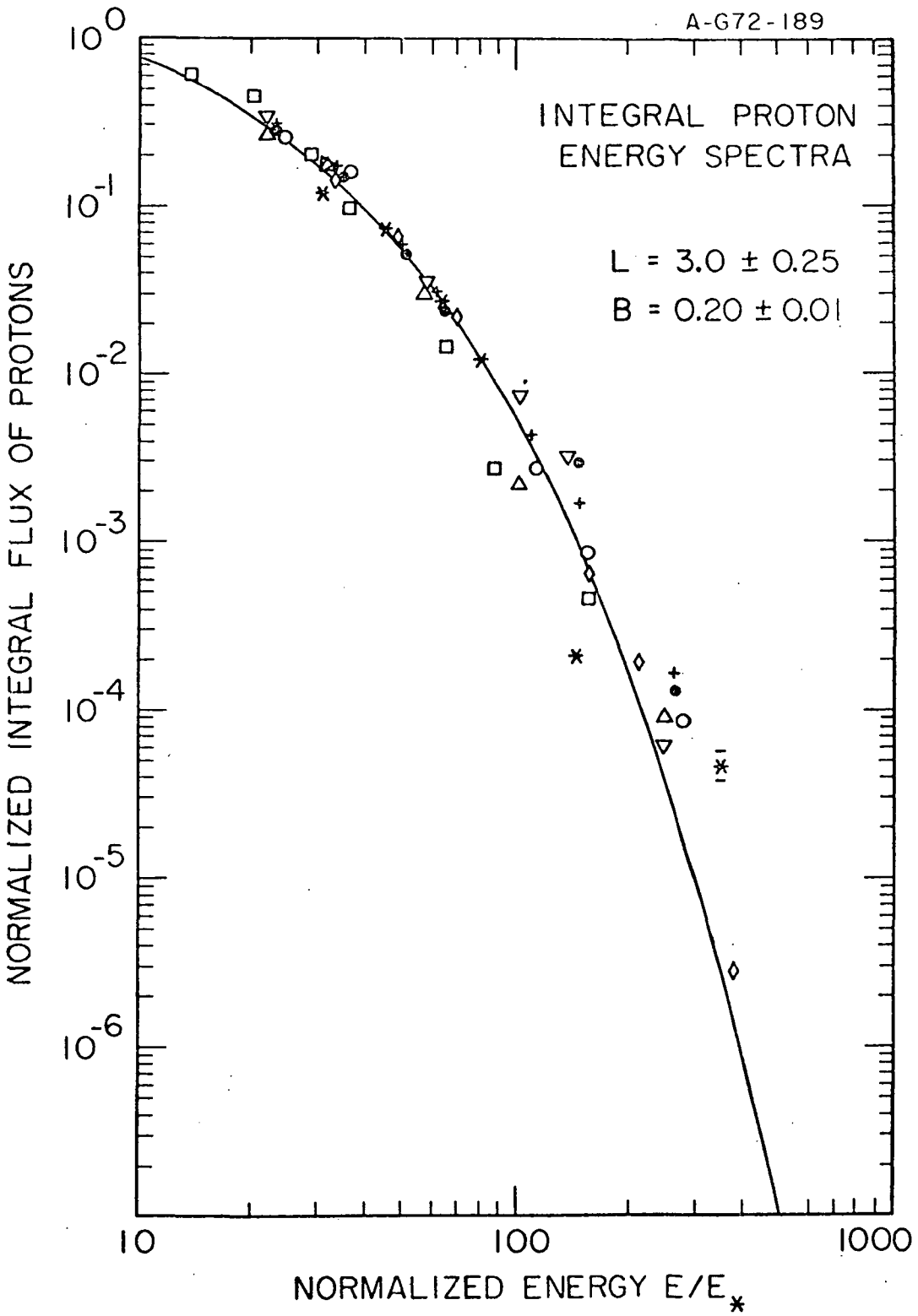
A-G72-189
INTEGRAL PROTON
ENERGY SPECTRA
L = 3.0 ± 0.25
B = 0.20 ± 0.01
NORMALIZED INTEGRAL FLUX OF PROTONS
NORMALIZED ENERGY E/E*
10^0
10^-1
10^-2
10^-3
10^-4
10^-5
10^-6
10
100
1000

Figure 18

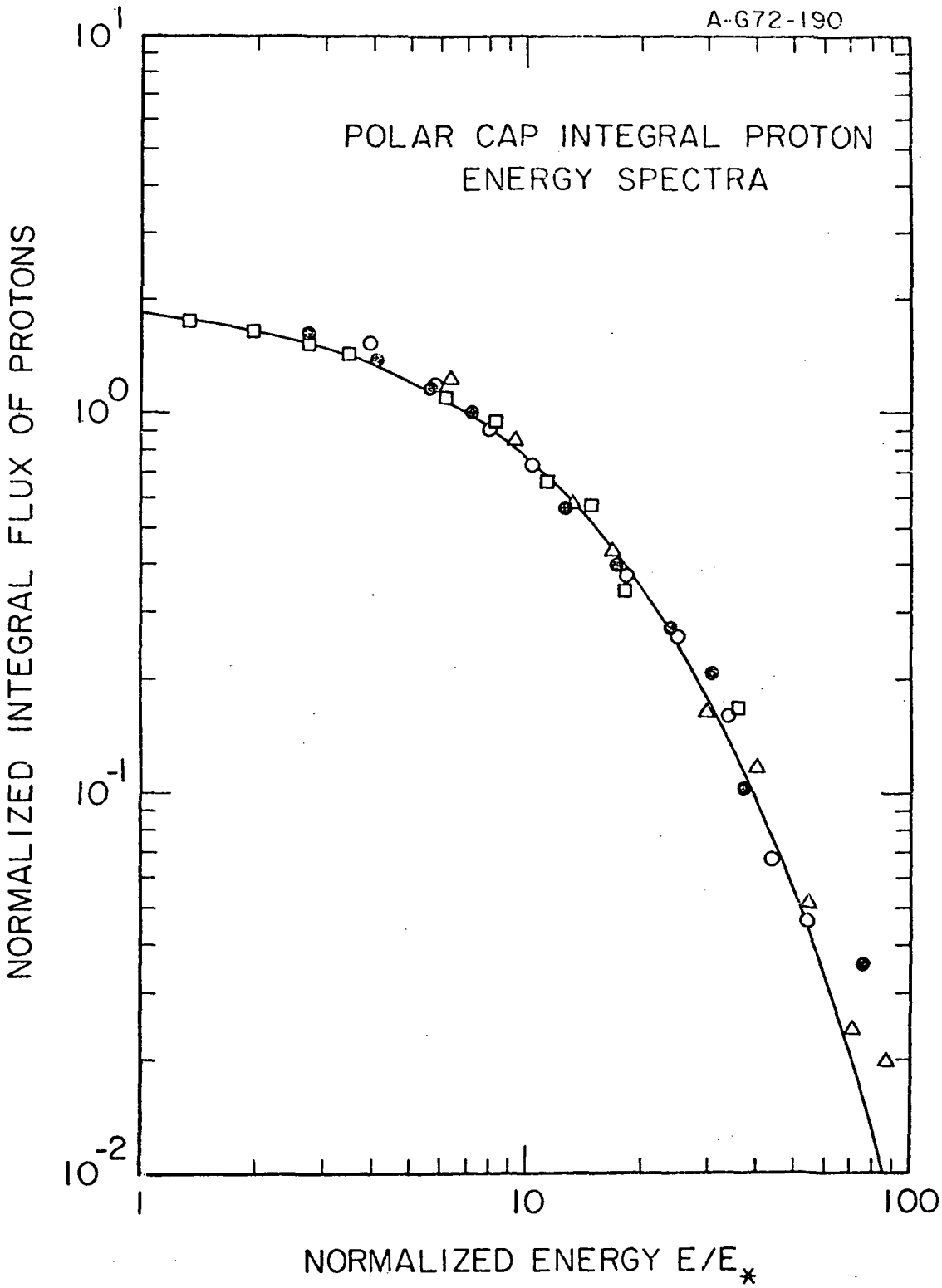
A-G72-190
POLAR CAP INTEGRAL PROTON
ENERGY SPECTRA
NORMALIZED INTEGRAL FLUX OF PROTONS
10^{1}
10^{0}
10^{-1}
10^{-2}
1
10
100
NORMALIZED ENERGY E/E_{*}

Figure 19

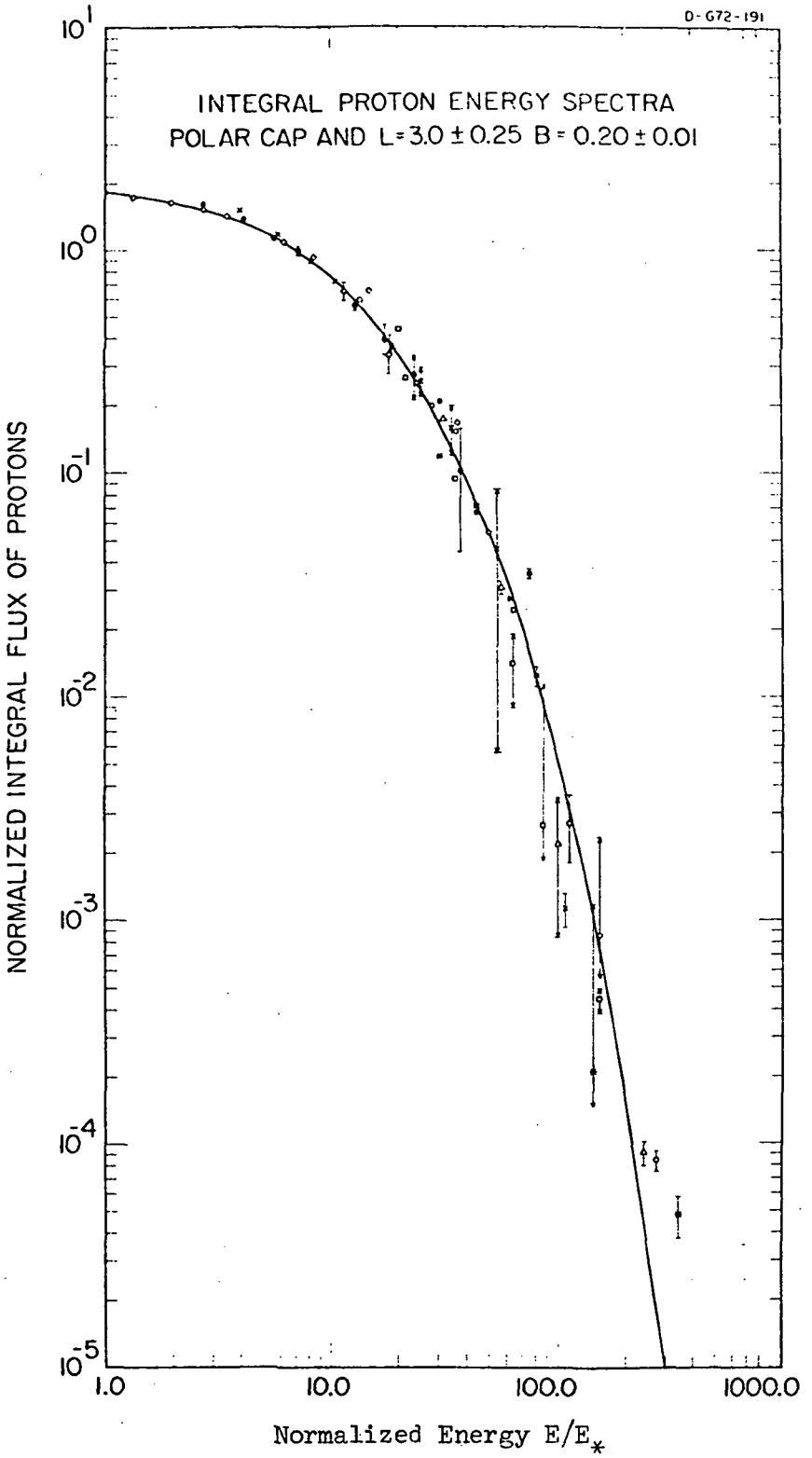
D-G72-191
INTEGRAL PROTON ENERGY SPECTRA
POLAR CAP AND L=3.0 ± 0.25 B = 0.20 ± 0.01
NORMALIZED INTEGRAL FLUX OF PROTONS
10^1
10^0
10^-1
10^-2
10^-3
10^-4
10^-5
1.0
10.0
100.0
1000.0
Normalized Energy E/E*

Figure 20

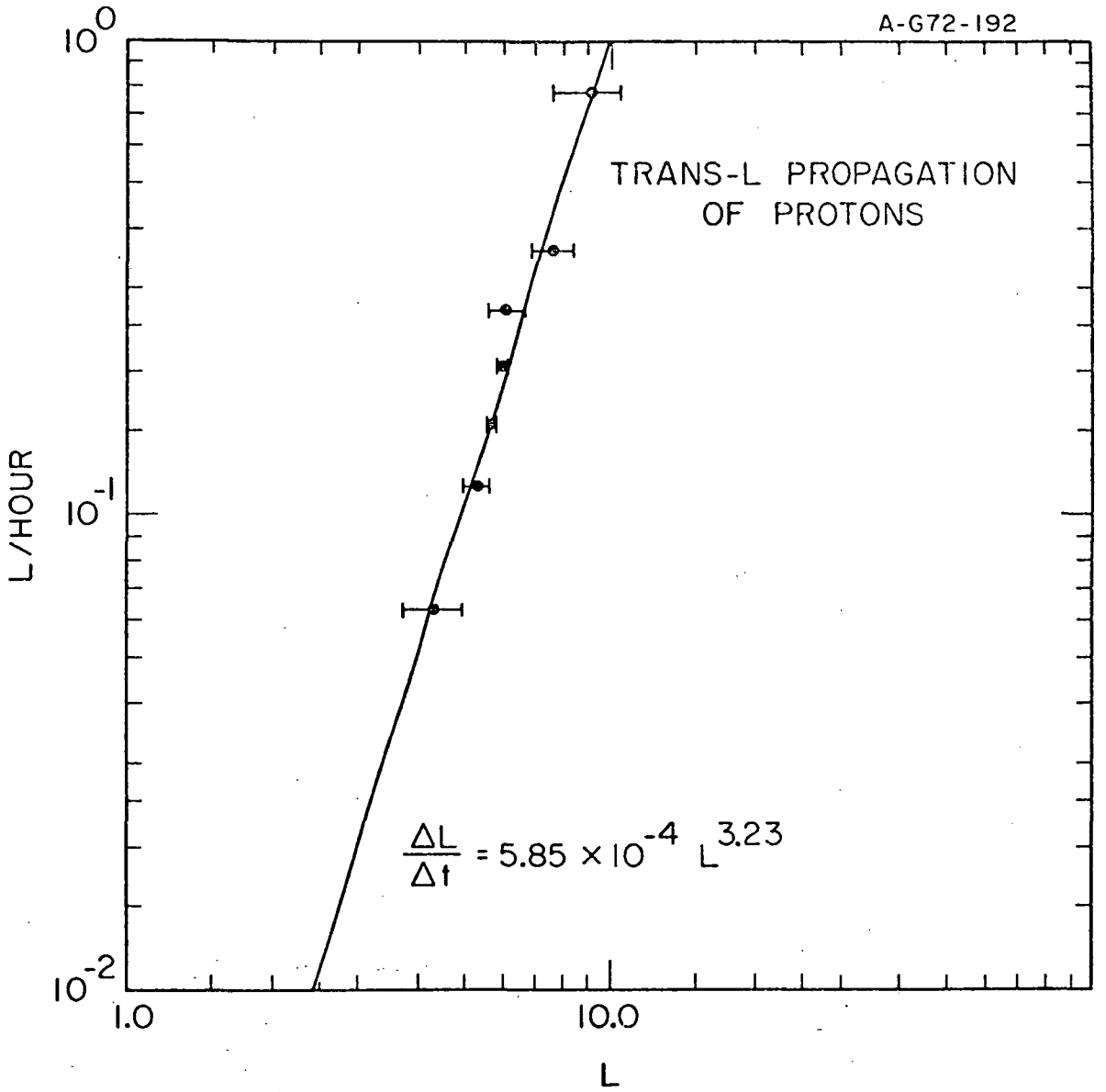
A-G72-192
TRANS-L PROPAGATION
OF PROTONS
$\frac{\Delta L}{\Delta t} = 5.85 \times 10^{-4} L^{3.23}$
L/HOUR
10^{0}
10^{-1}
10^{-2}
1.0
10.0
L

Figure 21

Unclassified

Security Classification

DOCUMENT CONTROL DATA - R&D

(Security classification of title, body of abstract and indexing annotation must be entered when the overall report is classified)

1 ORIGINATING ACTIVITY (Corporate author)

Department of Physics and Astronomy
University of Iowa
Iowa City, Iowa 52242

2a REPORT SECURITY CLASSIFICATION

Unclassified

2b GROUP

3. REPORT TITLE

Time Variations of Magnetospheric Intensities of Outer Zone Protons, Alpha Particles and Ions ($Z > 2$)

4. DESCRIPTIVE NOTES (Type of report and inclusive dates)

Ph.D. thesis, January 1973

5 AUTHOR(S) (Last name, first name, initial)

Bruce A. Randall

6. REPORT DATE	7a. TOTAL NO. OF PAGES	7b. NO. OF REFS
January 1973	71	39

8a. CONTRACT OR GRANT NO.	9a. ORIGINATOR'S REPORT NUMBER(S)
N00014-68-A-0196-0003	73-3
b. PROJECT NO.	
c.	9b. OTHER REPORT NO(S) (Any other numbers that may be assigned this report)
d.	

10. AVAILABILITY/LIMITATION NOTICES

Distribution of this document is unlimited

11. SUPPLEMENTARY NOTES	12. SPONSORING MILITARY ACTIVITY
	Office of Naval Research

13. ABSTRACT

See page 2.

DD FORM 1 JAN 64 1473

Unclassified

Security Classification

14. KEY WORDS	LINK A		LINK B		LINK C	
	ROLE	WT	ROLE	WT	ROLE	WT
Magnetospheric Protons						
Magnetospheric Alpha Particles						
Magnetospheric Ions						

INSTRUCTIONS

1. ORIGINATING ACTIVITY: Enter the name and address of the contractor, subcontractor, grantee, Department of Defense activity or other organization *(corporate author)* issuing the report.

2a. REPORT SECURITY CLASSIFICATION: Enter the overall security classification of the report. Indicate whether "Restricted Data" is included. Marking is to be in accordance with appropriate security regulations.

2b. GROUP: Automatic downgrading is specified in DoD Directive 5200.10 and Armed Forces Industrial Manual. Enter the group number. Also, when applicable, show that optional markings have been used for Group 3 and Group 4 as authorized.

3. REPORT TITLE: Enter the complete report title in all capital letters. Titles in all cases should be unclassified. If a meaningful title cannot be selected without classification, show title classification in all capitals in parenthesis immediately following the title.

4. DESCRIPTIVE NOTES: If appropriate, enter the type of report, e.g., interim, progress, summary, annual, or final. Give the inclusive dates when a specific reporting period is covered.

5. AUTHOR(S): Enter the name(s) of author(s) as shown on or in the report. Enter last name, first name, middle initial. If military, show rank and branch of service. The name of the principal author is an absolute minimum requirement.

6. REPORT DATE: Enter the date of the report as day, month, year; or month, year. If more than one date appears on the report, use date of publication.

7a. TOTAL NUMBER OF PAGES: The total page count should follow normal pagination procedures, i.e., enter the number of pages containing information.

7b. NUMBER OF REFERENCES: Enter the total number of references cited in the report.

8a. CONTRACT OR GRANT NUMBER: If appropriate, enter the applicable number of the contract or grant under which the report was written.

8b, 8c, & 8d. PROJECT NUMBER: Enter the appropriate military department identification, such as project number, subproject number, system numbers, task number, etc.

9a. ORIGINATOR'S REPORT NUMBER(S): Enter the official report number by which the document will be identified and controlled by the originating activity. This number must be unique to this report.

9b. OTHER REPORT NUMBER(S): If the report has been assigned any other report numbers *(either by the originator or by the sponsor)*, also enter this number(s).

10. AVAILABILITY/LIMITATION NOTICES: Enter any limitations on further dissemination of the report, other than those imposed by security classification, using standard statements such as:

(1) "Qualified requesters may obtain copies of this report from DDC."

(2) "Foreign announcement and dissemination of this report by DDC is not authorized."

(3) "U. S. Government agencies may obtain copies of this report directly from DDC. Other qualified DDC users shall request through _____."

(4) "U. S. military agencies may obtain copies of this report directly from DDC. Other qualified users shall request through _____."

(5) "All distribution of this report is controlled. Qualified DDC users shall request through _____."

If the report has been furnished to the Office of Technical Services, Department of Commerce, for sale to the public, indicate this fact and enter the price, if known.

11. SUPPLEMENTARY NOTES: Use for additional explanatory notes.

12. SPONSORING MILITARY ACTIVITY: Enter the name of the departmental project office or laboratory sponsoring *(paying for)* the research and development. Include address.

13. ABSTRACT: Enter an abstract giving a brief and factual summary of the document indicative of the report, even though it may also appear elsewhere in the body of the technical report. If additional space is required, a continuation sheet shall be attached.

It is highly desirable that the abstract of classified reports be unclassified. Each paragraph of the abstract shall end with an indication of the military security classification of the information in the paragraph, represented as *(TS), (S), (C), or (U)*.

There is no limitation on the length of the abstract. However, the suggested length is from 150 to 225 words.

14. KEY WORDS: Key words are technically meaningful terms or short phrases that characterize a report and may be used as index entries for cataloging the report. Key words must be selected so that no security classification is required. Identifiers, such as equipment model designation, trade name, military project code name, geographic location, may be used as key words but will be followed by an indication of technical context. The assignment of links, roles, and weights is optional.